TU Delft

Bsc. Thesis Applied Mathematics and Applied Physics

Modeling the behaviour of adsorbed chlorine atoms on a copper surface

PIETER VERSTRATEN

Delft University of Technology

Supervisors

Dr. J.M. Thijssen

Dr. ir. M.B. van Gijzen

Other Committee Members

Dr. A.F. Otte

Dr. J.L.A. Dubbeldam

August, 2017

Delft

Abstract

In the thesis of N. Batenburg unexpected domain boundary behaviour was observed for chlorine on a copper surface. The aim of this thesis is to create a model for the behaviour of adsorbed chlorine atoms on a copper surface, to better understand the domain boundary behaviour. The copper was cut along the (111) Miller plane, resulting in a hexagonal lattice. We present the Ising and the hard hexagon model before moving onto the full model used for the chlorine atoms on the copper surface.

For the final model first only two-point interaction was considered. It was found that the energy density of the domain walls found by N. Batenburg was higher than the energy density of other types of domain walls. Only when extreme values for the parameters are used, the energy density of the domain walls found by N. Batenburg become the lowest. However, when these parameters are used in a simulation, other configurations, which were not considered in the analysis, are found. We conclude that solely considering two-point interaction results in an inaccurate model, as the domain boundary behaviour found by N. Batenburg cannot be reproduced. An attempt was made to include three-point interaction, but due to a lack of time this attempt has not been successful. The three-point interaction has to be investigated further to create a more accurate model. Furthermore, the topology of the system could prove to be key to creating an accurate model.

Contents

1 Introduction

Materials are everywhere in the world, think about the wood of a table, but also the copper used in wires. For the progress of technology it is of vital importantce to fully understand the behaviour of the used materials. This allows us to create smaller, better and new devices. To understand the behaviour of a material, we have to get down to the atomic scale. We can describe the behaviour of a single atom using quantum mechanics. Quantum mechanics can still be used to describe a group of atoms. However, when we want to describe the behaviour of a large collective of atoms, we have to get down to the atomic scale and study the behaviour of this collective.

The starting point of this research is the Bsc thesis of N. Batenburg [2]. In this work the behaviour of adsorbed chlorine atoms on a copper surface was studied. This was done using a scanning tunneling miscroscope in Otte lab. Chlorine atoms form domains on the copper surface and unexpected domain boundaries were observed. This thesis aims to create an accurate model for the behaviour of adsorbed chlorine atoms on a copper surface, to better understand the domain boundary behaviour. If this model is able to produce the same kind of domain boundary behaviour, it may be possible to understand how and why this behaviour occurs.

Before this model is created, two other models will be investigated. These models are the Ising model and the hard hexagon model. For all three models the Monte Carlo method will be used. The Ising model will give a good insight into a statistical mechanics model. Furthermore, we shall investigate the convergence of a Monte Carlo simulation using the Ising model. The hard hexagon will function as a starting model for the model we are trying to create. It will introduce the adsorption and diffusion of atoms on a surface. Furthermore, it is formulated on a triangular lattice, which has its resemblance with the hexagonal lattice used in the final model. For the final model we shall first only consider two-point interaction, but later also include three-point interaction.

This thesis starts with a discussion of the geometry of the copper crystal and the chlorine adsorption process in Chapter 2. Then the results found by N. Batenburg are briefly discussed in Chapter 3. Using the knowledge from these two chapters we shall formulate the problem that will be investigated in this thesis in Chapter 4. The Monte Carlo method will be discussed in Chapter 5. Then the models will be investigated, first the Ising model in Chapter 6, then the hard hexagon model in Chapter 7 and finally we create a model for the behaviour of adsorbed chlorine atoms on a copper surface in Chapter 8. Finally, conclusions are drawn and suggestions for further improvements of the model are made in Chapter 9.

2 Copper crystal and chlorine adsorption sites

In this chapter we discuss the geometry of the copper crystal and the geometry of the copper surface where the chlorine atoms are adsorbed. This knowledge is necessary to understand the problem investigated in this thesis.

For the copper crystal we can assume to good approximation that the atoms behave like attracting hard spheres. For minimal energy the spheres assume a close-packed structure. Such a structure consists of layers with a triangular arrangement of the copper atoms. Figure 2.1 shows one layer of a close-packed structure. For each layer all spheres must be in equivalent positions, so all spheres shall be on positions of one of the three lattices, denoted as A, B or C. In this layer all spheres are in position A. The centers of the upward-pointing triangles are the B sites and the centers of the downward-pointing triangles are the C sites. The layer below the A atoms shall either occupy the B or the C sites. The next layer can then occupy the A sites again, leading to an ABABAB... or ACACAC... stacking. Alternatively, the next layer can also occupy the sites which have not yet been used. We obtain an ABCABCABC... or ACBACBACB... stacking. The former is called a *hexagonal close-packed*, or hcp structure. The latter is called a *face-centered cubic*, or fcc structure. Copper assumes an fcc structure. Fcc and hcp both achieve the highest average density, $\frac{\pi}{3\sqrt{2}} \approx 0.74048$ [5].

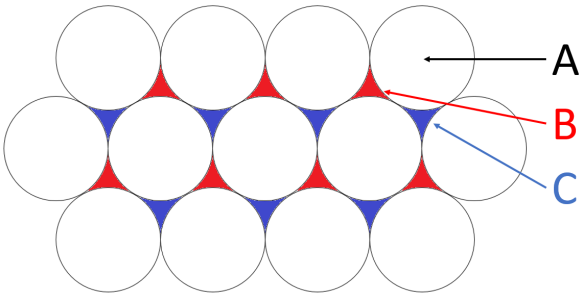

Figure 2.1: A close-packed layer of spheres. These spheres occupy positions A. The layers above and below can occupy positions B or C.

The copper crystal can be cut along several directions, resulting in different copper surfaces. To specify the direction of the cutting, *Miller planes* are commonly used. If we take a cube as in Figure 2.2 then the $(u\ v\ w)$ Miller plane is the plane through the points $(\frac{\mathbf{a}}{u}, 0, 0)$, $(0, \frac{\mathbf{b}}{v}, 0)$ and $(0, 0, \frac{\mathbf{c}}{w})$. [6]

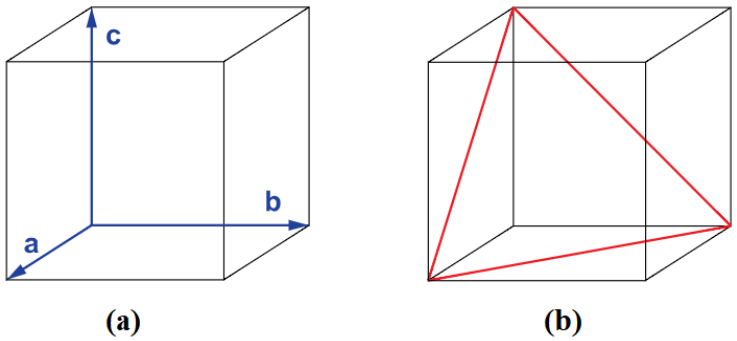

Figure 2.2: **(a)** Cubic lattice with lattice vectors **a**, **b** and **c**. In this figure all vectors have the same length. **(b)** A (111) Miller plane.

For the experiment, as conducted by N. Batenburg, a copper crystal was cut along the (111) Miller plane. This yields a a two-dimensional hexagonal surface as in Figure 2.3[1], which can be referred to as Cu(111). [2]

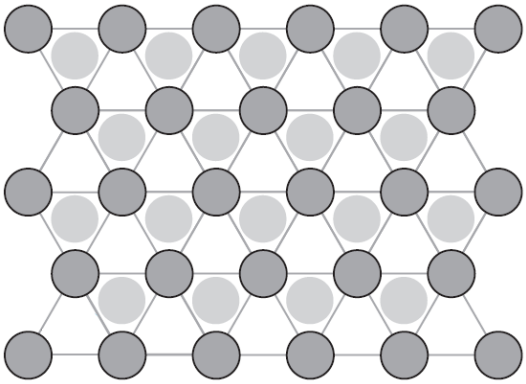

Figure 2.3: The hexagonal lattice obtained by cutting a copper crystal along the (111) Miller plane. The lattice of the surface layer is occupied by the dark gray spheres, the lattice of the layer below is occupied by the light gray spheres and the third layer is left blank.

The chlorine atoms can be adsorbed on several adsorption sites on the copper surface. It can be adsorbed on the site where normally the next copper atom would be, this is called the fcc hollow site. It could also be adsorbed on top of a copper atom in the first layer underneath the surface, this is called the hcp hollow site. A chlorine atom can also be adsorbed on top of a copper atom of the top layer. Finally it can be adsorbed on the bridge between two copper atoms of the top layer. These four types of adsorption sites are shown in Figure 2.4. [9]

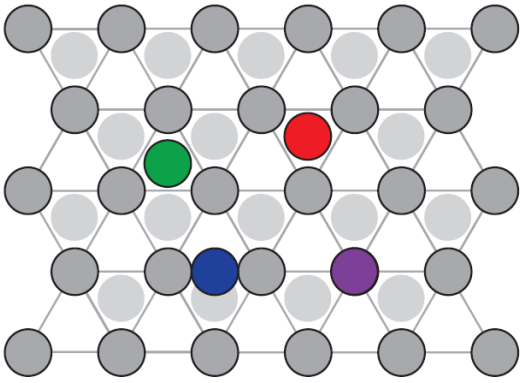

Figure 2.4: The four types of adsorption sites. Red is the fcc hollow site, green is the hcp hollow site, blue is the bridge between two copper atoms and purple is on top of a copper atom.

These are the four adsorption sites on a perfect copper surface. When the copper surface is not perfectly flat, there are regions with extra layers of copper. Chlorine atoms can be adsorbed at the step edge of these two regions.

Different adsorption sites have different adsorption energies, these are listed in Table 2.1. [9] These energies are for single chlorine atoms placed on a copper surface. As the bridge and on top adsorption sites are energetically unfavorable we would expect only the fcc and hcp

[1]Figures 2.3, 2.4, 2.6, 3.1, 3.2 and 3.3 have been taken from the thesis of N. Batenburg

Table 2.1: The adsorption energies for five types of adsorption sites.

Type of adsorption site	**Adsorption energy, eV**
fcc holow site	-1.831
hcp hollow site	-1.824
bridge	-1.752
on top	-1.442
step edge	-2.126

hollow sites to be occupied on a perfectly flat surface with no step edges. An example of a chlorine surface reconstruction is shown in Figure 2.5 as found by Goddard and Lambert [4].

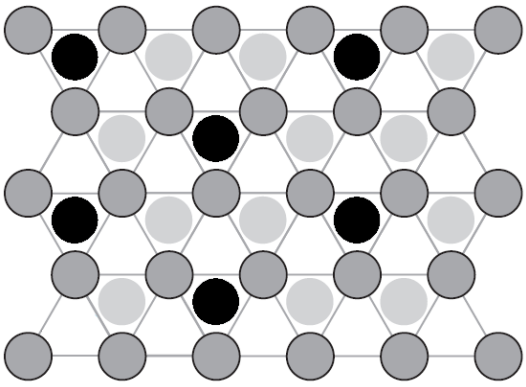

Figure 2.5: A chlorine surface reconstruction on a Cu(111) surface as found by Goddard and Lambert. The black sites are occupied by the chlorine atoms.

There exist six non-equivalent domains as in Figure 2.5. Three of these domains occupy fcc hollow sites and the other three occupy the hcp hollow sites. The three fcc domains can be found in Figure 2.6a, the three hcp domains in Figure 2.6b and the six non-equivalent domains in Figure 2.6c.

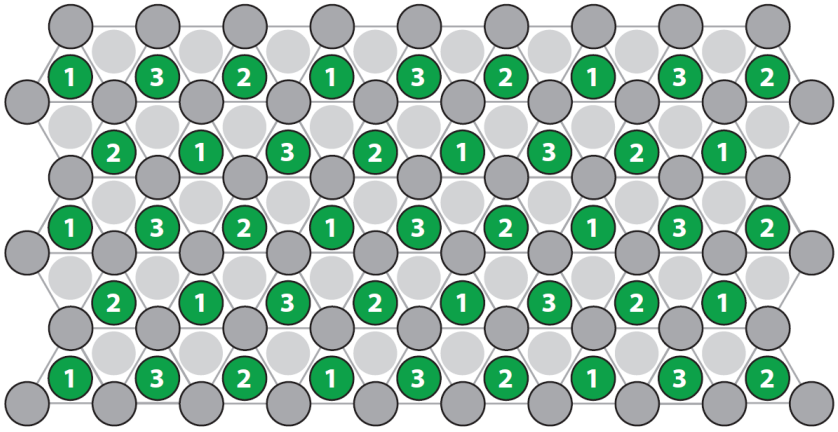

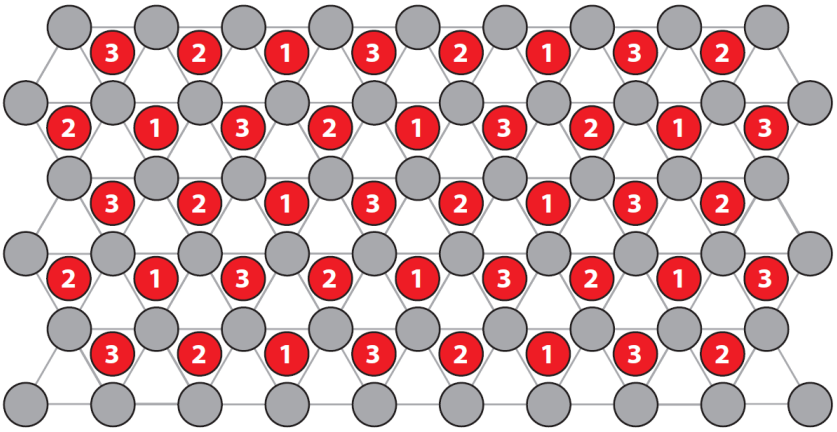

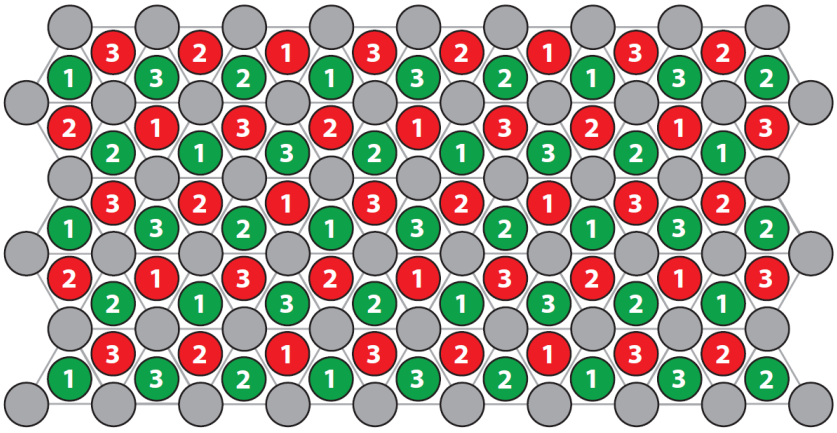

Figure 2.6: **(a)** The three non-equivalent fcc domains. **(b)** the three inequivalent hcp domains. **(c)** the six inequivalent domains.

3 Chlorine domain boundary behaviour

This chapter shall briefly discuss the results found by N. Batenburg. [2] The scans shown in this chapter, Figures 3.1 and 3.3, were made using a scanning tunneling microscope.

Chlorine was adsorbed on a Cu(111) surface, resulting in domains of chlorine on the fcc lattices as in Figure 2.6. The domains occupy the fcc lattice, since the fcc hollow sites are energetically more favorable compared to the hcp hollow sites, as can be found in Table 2.1. It would be energetically most favorable to have a single domain which occupies one of the three fcc lattices from Figure 2.6a. However, at the start there is an empty Cu(111) surface and multiple domains form. These domains can occupy different fcc lattices as they do not know what lattice the other domains occupy. When the domains meet, it costs too much energy to shift one of the two domains to the other fcc lattice. Due to this a local minimum is found in the form of domain walls. A scan which shows straight and irregular domain walls can be seen in Figure 3.1. [2] The bright points indicate the presence of a chlorine atom. The area in Figure 3.1 is mostly occupied by chlorine atoms, however there are some dark spots which indicate vacancies. There are also some bright lines, these are the straight domain walls. The density of chlorine atoms is higher here, resulting in a brighter image.

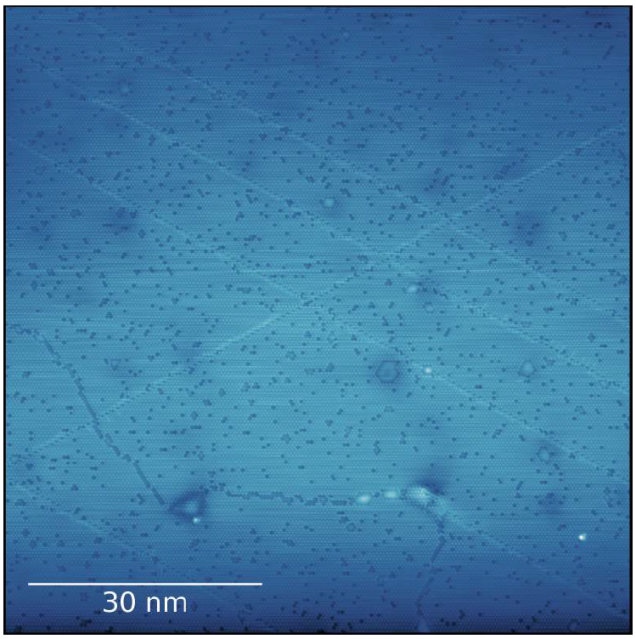

Figure 3.1: Straight and irregular domain walls on a chlorine-reconstructed Cu(111) surface.

The domain walls are stable, propagating in the same direction even when crossing each other or when encountering a step edge. In the thesis of N. Batenburg six different types of straight domain walls were recognized, which can be seen in Figure 3.2. When the distance between two chlorine atoms becomes too small, the atoms repel each other. Due to this a certain distance between the two domains exists. It would theoretically be possible to have no chlorine atoms between the two domains, resulting in a domain wall which exists of vacancies. However, as can be concluded from the results found by N. Batenburg, it is more favorable to have the chlorine atoms occupy the hcp positions between two domains.

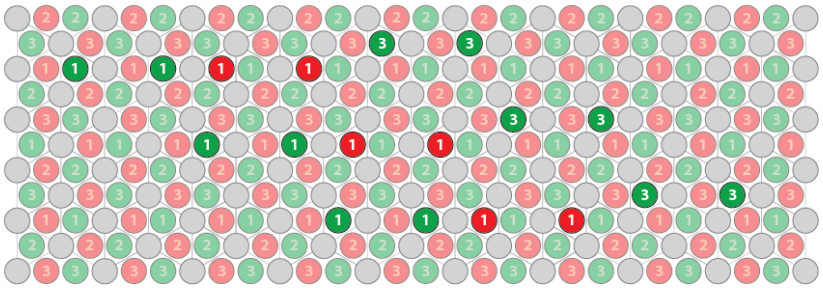

(a)

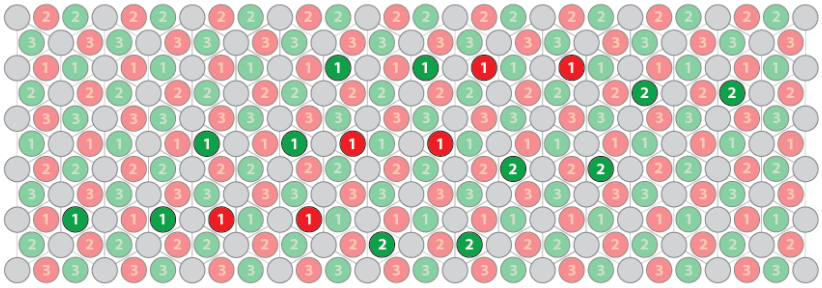

(b)

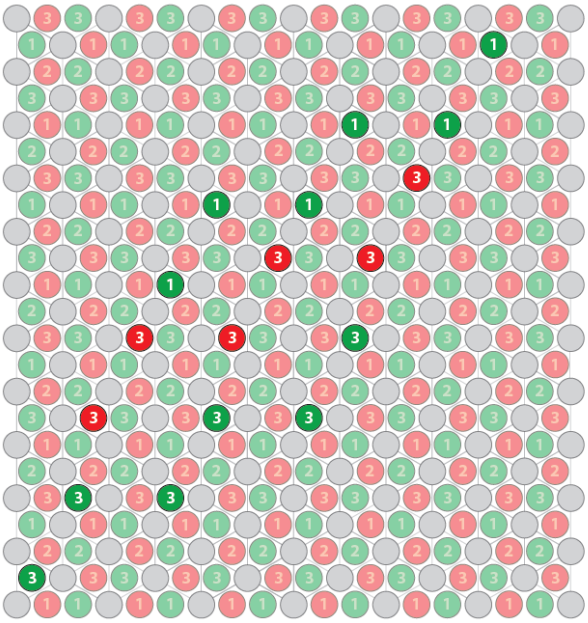

(c)

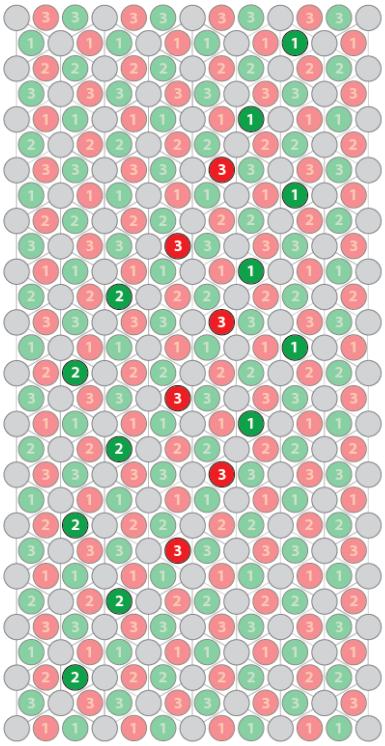

(d)

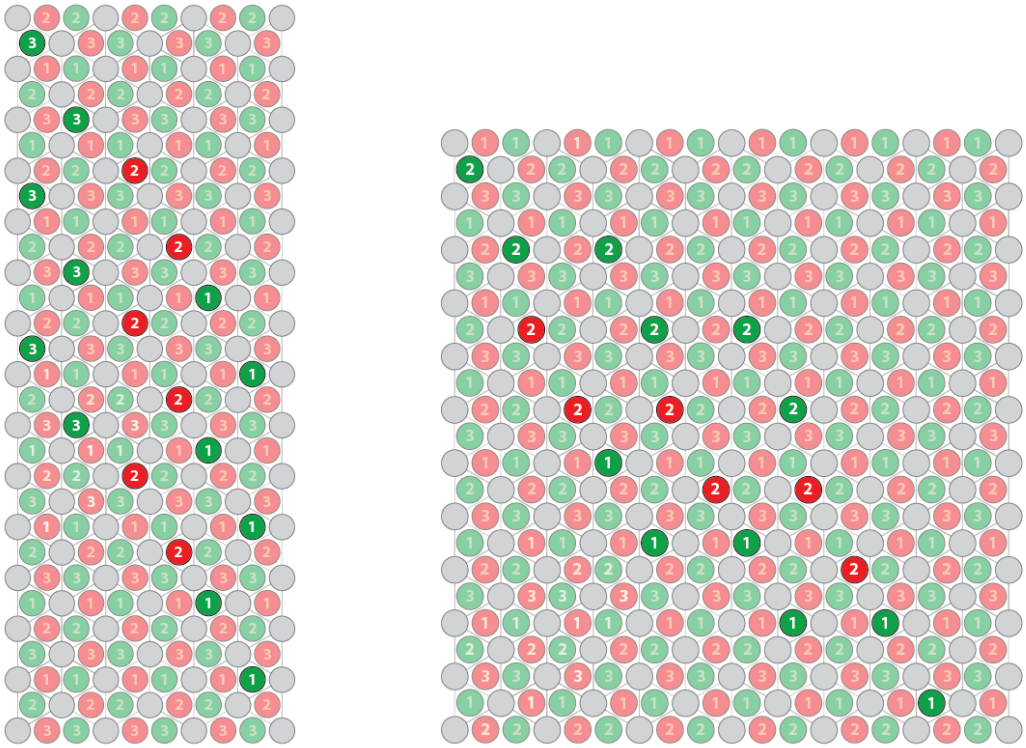

Figure 3.2: The six different types of straight domain walls as recognized by N. Batenburg.

An interesting feature of the studied system is the presence of *screw dislocations*. These are cause by defects in the underlying copper crystal. Instead of a discontinuity in height as with a step edge, the surface is continuously warped. As a result, one can move from a domain situated on an fcc lattice to another fcc lattice without crossing a domain wall. An example of a screw dislocation can be found in Figure 3.3 [2]. Furthermore, one can see that two domain walls originate from the screw dislocation.

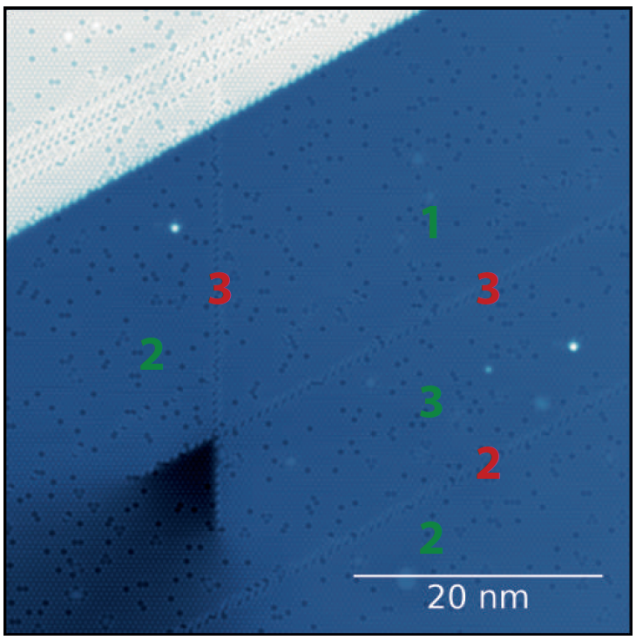

Figure 3.3: An example of a screw dislocation. One can move from the domain occupying the left fcc 2 lattice to the domain occupying the fcc 3 lattice without crossing a domain wall. Two domain walls originate from the screw dislocation.

4 Problem analysis

In Chapter 2 the geometry of the copper crystal and the chlorine adsorption sites were discussed. In Chapter 3 the results of N. Batenburg were briefly discussed. In this chapter we shall formulate the problem investigated in this thesis. Furthermore, the approach to solving the problem shall be discussed.

In this thesis we want to investigate the nature of the domain walls as found by N. Batenburg. Under which circumstances do the domain walls appear, and is it possible to control which kind of domain walls exist? This will be done by creating a model of the investigated system. Before this model is created, two other models will be investigated, the Ising model and the hard hexagon model. Each of the three models will use the Monte Carlo method. In the next chapter the Monte Carlo method will be discussed. In Chapters 6 and 7 the Ising and hard hexagon models are discussed. Using the knowledge from these chapters we shall develop a model to investigate the domain walls on a chlorine-reconstructed Cu(111) surface in Chapter 8.

5 Monte Carlo method

The Monte Carlo method has several uses. It can be used to calculate integrals, this is especially useful when integrating over high-dimensional volumes. However, the Monte Carlo method is mostly used in statistical mechanics. Due to the fact that statistical mechanics considers a lot of degrees of freedom, it is very time consuming to solve equations of motion for each of the particles considered in the system. These methods do exist, an example is molecular dynamics simulations. An advantage of molecular dynamics is that the process is modeled in real time. For many Monte Carlo simulations the time in the process is not the same as real time. The Monte Carlo method used in this thesis is *kinetic Monte Carlo*. Kinetic Monte Carlo offers a way to keep track of real time during a simulation. In contrast to molecular dynamics, kinetic Monte Carlo focuses on the "interesting" processes as we shall see later in this chapter. An introduction into the method can be found in the PhD thesis of J. Rogal [11].

As mentioned in the previous chapter, we shall use the Monte Carlo method for the models discussed in this thesis. In this chapter we shall first consider Markov chains, then we shall discuss the kinetic Monte Carlo method and finally we shall investigate how to measure the convergence of a Monte Carlo method.

5.1 Markov chains

Kinetic Monte Carlo simulates how a system moves from one state to another. Each transition is one kinetic Monte Carlo step. These transitions are called rare events, since the time between two transitions is very long on the time scale of atomic vibrations. Due to this the system has no memory of how it has arrived at a certain state. This causes each transition to be independent from the other transitions. Thus, when the system is in state S_i, the probability of transitioning to state S_j is independent of the states the system was in before state S_i. Such a sequence of states is called a Markov chain, named after the Russian mathematician Andrey Markov. The probability of going from state S_1 to S_2, from S_2 to S_3, and so on until state S_N, is given by

$$P_N(S_1, S_2, \ldots, S_N) = P_1(S_1)T(S_1 \to S_2)\ldots T(S_{N-1} \to S_N) \tag{5.1}$$

$P_1(S_1)$ is the probability to be in S_1 and $T(S_i \to S_{i+1})$ is the probability to transition from state S_i to state S_{i+1}. This transition probability is normalized,

$$\sum_{S'} T(S \to S') = 1 \tag{5.2}$$

Thus, the probability to move to any state is 1 as we would expect. An example of a Markov chain is the random walk on a square lattice. Consider a square lattice with a single particle on the lattice as in Figure 5.1. In each state the particle is on a certain square. From this square it can move to one of the neighbouring squares. These transitions all have probability $\frac{1}{4}$. These probabilities are not affected by the history of the walk. Note that Eq. (5.2) is satisfied.

A non-Markovian process is a stochastic process which has memory. As an example of a non-Markovian process we modify the random walk. We do not allow the particle to move to a square which it has visited before. Clearly, when in state S_i, the probability to transition to state S_j can be influenced by previous states, as the history can change the probability from $\frac{1}{4}$ to 0. This process is called a self-avoiding walk and it is relevant in two-dimensional polymer physics, as a polymer cannot overlap. [12]

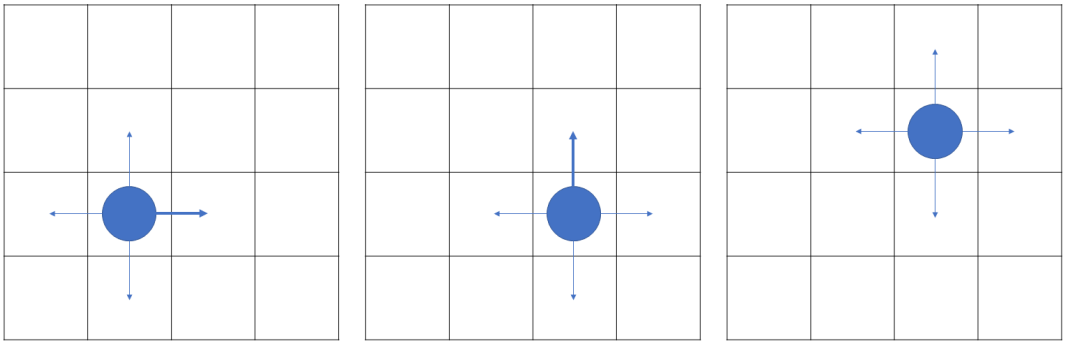

Figure 5.1: An example of a random walk. The transition of state 1 to state 2 is by moving to the right and the transition of state 2 to state 3 is by moving up.

Let us denote the probability of being in state S_j at time t by $P(S_j, t)$. The change of $P(S_j, t)$ in time is governed by two processes:

1. Being in state S_j at time t and moving to another state S_i at time $t+1$. This will lead to a decrease in $P(S_j)$. The probability of this happening is given by $P(S_j, t)T(S_j \to S_i)$, thus the probability to be in state S_j at time t multiplied by the probability of moving from S_j to S_i.
2. Being in some state S_i at time t and moving to state S_j at time $t+1$. This will lead to an increase in $P(S_j)$. The probability of this happening is given by $P(S_i, t)T(S_i \to S_j)$.

Summing over all states i leads to the *master equation*

$$P(S_j, t+1) - P(S_j, t) = -\sum_i P(S_j, t)T(S_j \to S_i) + \sum_i P(S_i, t)T(S_i \to S_j) \tag{5.3}$$

In thermal equilibrium the probability to be in a certain state must be constant, thus the following must hold

$$P(S_j, t+1) = P(S_j, t)$$

This is equivalent to requiring

$$\sum_i P(S_j, t)T(S_j \to S_i) = \sum_i P(S_i, t)T(S_i \to S_j)$$

A particular solution is given by (we omit the time dependence of P)

$$P(S_j)T(S_j \to S_i) = P(S_i)T(S_i \to S_j) \tag{5.4}$$

Eq. (5.4) must hold for all pairs of S_i and S_j. This is called the *detailed balance solution*. When Eq. (5.4) holds, the expected number of transitions from S_j to S_i is equal to the expected number of transitions from S_i to S_j for every pair of S_i and S_j, keeping the system in equilibrium. [12]

5.2 Kinetic Monte Carlo

An example of a rare event that is important in this thesis, is the diffusion of a chlorine atom on the copper surface. A particle on a surface vibrates around its equilibrium position about once every picosecond, whereas diffusion happens on the time scale of microseconds. Thus a particle vibrates about 10^9 times before it diffuses, making diffusion a good example of a rare event. Using molecular dynamics to simulate diffusion, would require to first simulate

10^9 vibrations before the particle diffuses. Due to this it is not possible to directly simulate a lot of diffusion processes. We are interested in diffusion and not in the vibrational dynamics of a particle, so molecular dynamics is not useful in this case. Instead we shall use kinetic Monte Carlo, which focuses on the diffusion and not on the vibration of the particle.

For a kinetic Monte Carlo simulation a list of all possible processes has to be made. An example of a process is the adsorption of an atom on a surface. Another process would be the diffusion of this atom on the surface. Each process p has a certain rate r_p. Define $R = \sum_p r_p$ as the total rate. This is the number of processes that occur per unit of time. Starting at an initial state a process k is chosen randomly by

$$\sum_{p=0}^{k-1} r_p \leq \rho_1 R \leq \sum_{p=0}^{k} r_p \tag{5.5}$$

ρ_1 is a random number between 0 and 1. If r_p is very large compared to r_q, then the probability of choosing process p is much larger than the probability of choosing process q. After a process k has been chosen, it shall be executed. The kinetic Monte Carlo algorithm simulates a Poisson process, such that we can keep track of real time. The time between two events in a Poisson process can be calculated using the exponential distribution. To generate exponential variates we use Eq. (5.6). T is the time between two events, ρ_2 is a random number between 0 and 1, and R is the total rate which has previously been introduced.

$$T = -\frac{\ln(\rho_2)}{R} \tag{5.6}$$

If we take t as the real time, then we can keep track of real time by updating t every time we execute a certain process using Eq. (5.7)

$$t \to t - \frac{\ln(\rho_2)}{R} \tag{5.7}$$

In some models the rates r_p can change during the simulation. If this is the case, then the rates have to be updated after a process is executed. [11]

In many cases the rates in a kinetic Monte Carlo simulation depend on energy. If it is possible to map the investigated model on a lattice, such as the lattices we have seen in Chapter 2, then a *Lattice Gas Hamiltonian* can be developed. This Hamiltonian depends on on-site energies F_i^0 and the interactions between different lattice sites V. This results in a Hamiltonian as in Eq. (5.8).

$$\mathcal{H} = \sum_i n_i F_i^0 + \sum_{ij} V_{ij} n_i n_j + \sum_{ijk} V_{ijk} n_i n_j n_k + \dots \tag{5.8}$$

$n_i = 0$ when site i is not occupied and $n_i = 1$ when site i is occupied. V_{ij} is the interaction between particles on site i and site j. V_{ijk} is the interaction between particles on sites i, j and k. These are two-point and three-point interaction respectively, also called pair-interaction and trio-interaction. The interaction parameters are symmetric, $V_{ij} = V_{ji}$. [11] For each model a choice has to be made which kind of interactions are taken into account. In some cases pair-interaction may be enough to accurately describe a system, however it is also possible that more types of interaction are necessary.

5.3 Convergence of a Monte Carlo simulation

The convergence of an algorithm plays a major role in numerical analysis. It is desirable that an algorithm converges quickly to reduce computation time. When computing an integral an algorithm converges to a certain number. In our case the simulations should converge

to a certain state. We shall first discuss to what state a system should converge. Then we shall see how this convergence can be measured.

For most statistical systems the behaviour is determined by the energy of the system, as the system strives for a minimal energy. If an integral exists, then it has a definite value. It can be difficult to determine the value, but we know for certain that there do not exist two different values, such that the integral is equal to both values. This is different for a statistical system. States can be *degenerate*, this means that the states are different, but they correspond to the same energy. If the behaviour is solely determined by the energy of states, then the system will not prefer one of these states over the other. In contrast to an integral, a system does not necessarily converge to a certain state.

Consider the hypothetical potential in Figure 5.2a. The system will converge to a state with one of the minima, however it does not prefer one of the states, as long as it has a minimal energy. Due to this is not certain to which minimum the system will converge. Furthermore, the system is not necessarily stuck in a minimum. With enough thermal fluctuations the system can transition to another minimum. In Figure 5.2b a potential with two unequal minima is shown. The system favours the global minimum over the local minimum on the left. However, it is still possible that the system converges to a state corresponding to the local minimum on the left. This occurs when the system does not have enough energy to cross the barrier between the two minima.

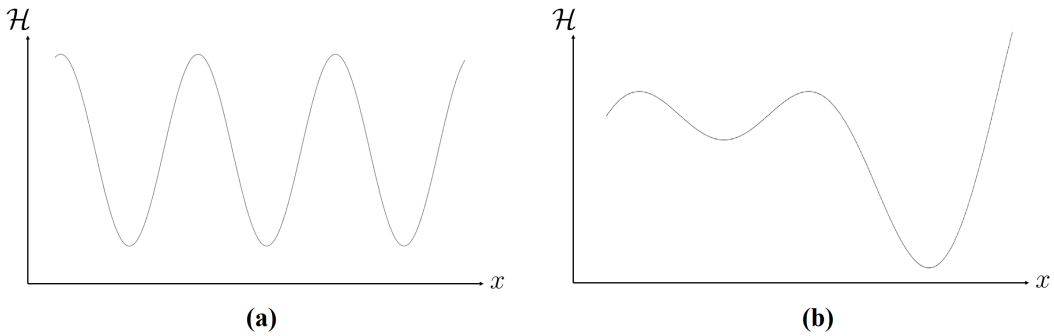

Figure 5.2: **(a)** A potential with a sequence of equal minima. **(b)** A potential with two unequal minima.

To measure the convergence of the kinetic Monte Carlo one chooses a property of the system, for example energy, and measures this property throughout the simulation. Normally, there is an exponential behavior with a certain time constant τ. For large τ the convergence is slow, for small τ the convergence is fast. This τ can be determined by fitting an exponential for the data gathered by measuring the chosen property for every state.

As an example we shall consider the hypothetical situation in Figure 5.3. The energy of the system was measured throughout time. This was done for different sizes of the system. The dependence between the size of the system and τ can be deduced by looking at Table 5.1. When N becomes twice as large, τ becomes four times as large. When N becomes three times as large, τ becomes 9 times as large. We conclude that $\tau \propto N^2$. We shall use the same procedure in this example for the Ising model, however the results may be different.

Table 5.1: The different time constants τ for the three different sizes of the system N for the hypothetical situation from Figure 5.3

Size of the system, N	**Exponential time constant, τ**
100	5
200	20
300	45

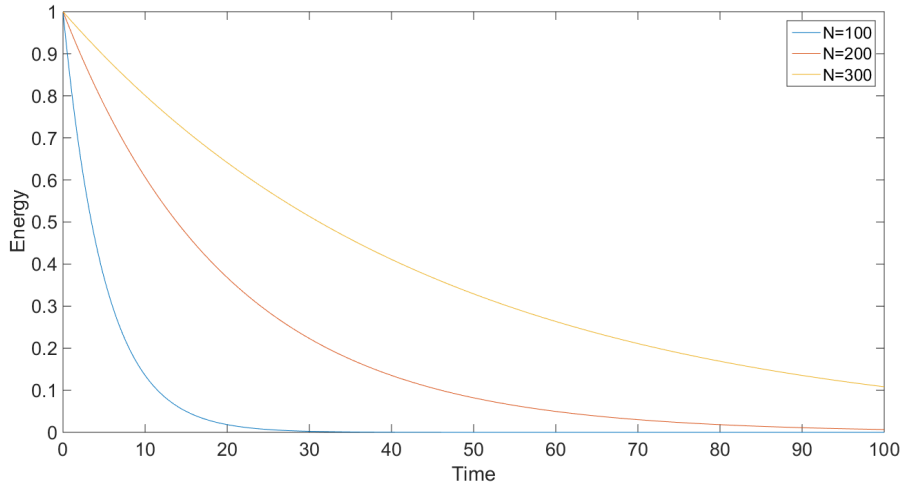

Figure 5.3: A hypothetical situation in which the energy of the system is measured throughout time for different sizes of the system. As the size of the system increases, τ increases as well.

Following this procedure, one can establish the convergence of a kinetic Monte Carlo simulation. In this case the convergence was based on differing the size of the system. The convergence can also be based on other parameters. It is important that only the chosen parameter is varied, while the other parameters are kept constant.

This concludes the chapter of the Monte Carlo method. In the next chapters the Ising model and the hard hexagon model shall be investigated. Finally, a model for the problem as established in Chapter 4 will be created. In all cases the Monte Carlo method will be used. Furthermore, the convergence of the Ising model shall be investigated.

6 Ising model

This chapter shall discuss the Ising model. The Ising model is a famous model in statistical mechanics. It can describe various processes, of which the most common is ferromagnetism. Another process that it can describe is the process of atoms being adsorbed on surfaces. In general this model is applicable to any process where there are only two values possible for a degree of freedom. [12]. In this chapter we only consider the two-dimensional Ising model. First a description of the Ising model is given. Then an analysis of the model follows. Next it is discussed how this model can be simulated. Finally, the convergence of the Ising model is investigated. Information about the Ising model can be found in many statistical mechanics books, see for example references [7], [10] and [12].

6.1 Description of the Ising model

The two-dimensional Ising model is formulated on a square lattice of size $L \times L$. Every site is labelled by i, with $i = 1, 2, \ldots, L^2$. Each site has a variable s_i. When the Ising model is used to describe ferromagnetism s_i represents the spin of a site. When the process of atoms adsorbed on surfaces is described, s_i represents whether a site is occupied or not. For every case s_i can take two values and for simplicity we shall take $s_i = \pm 1$. $s_i = +1$ denotes an up spin in the case of ferromagnetism or occupied in the case of atoms adsorbed on surfaces. $s_i = -1$ denotes a down spin or not occupied. From now on we shall take s_i to represent the spin of sites. The energy for a certain configuration of spins is given by the following Hamiltonian

$$\mathcal{H} = -K \sum_{\langle i,j \rangle} s_i s_j - H \sum_i s_i \tag{6.1}$$

$\langle i, j \rangle$ represents two nearest neighbours. Every site has four nearest neighbours, the one above, the one below, the one to the left and the one to the right. K is a coupling constant between the nearest neighbours and H is the magnetic field.

Since at low temperatures low energies are favoured, we now consider which configuration corresponds to a low energy. For the first sum in Eq. (6.1) we note that like nearest neighbours lower the energy when $K > 0$. It does not matter whether the spins are positive or negative, as long as they are equal. When $K < 0$, the energy is lowered by having unlike nearest neighbours. We expect ferromagnetism for $K > 0$ and antiferromagnetism for $K < 0$. For the second sum we note that for positive H the spins should have the value $+1$ to lower the energy and for negative H the spins should have the value -1 to lower the energy. In general, the spins favour pointing in the same direction as the magnetic field and direct neighbours preferably point in the same direction.

To minimize the influence of boundaries, periodic boundary conditions are used. This means that for a spin at the border, the direct neighbour is at the other side of the lattice. An example is shown in Figure 6.1. Since there is no direct neighbour to the left for the chosen spin, instead the neighbour at the far right is chosen as direct neighbour.

This concludes the description of the two-dimensional Ising model. In the next subsection, several properties of this model will be analyzed.

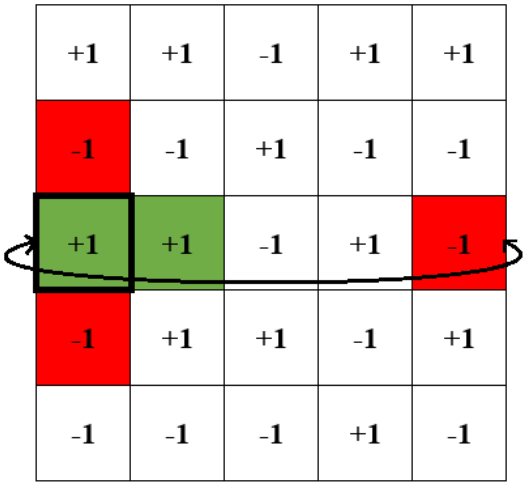

Figure 6.1: A 5×5 lattice filled randomly with ± 1. The colors show the nearest neighbours for a spin at the border. One direct neighbour has the same spin value, indicated with the colour green. Three have a different spin value, indicated in red. The left neighbour of the selected spin is on the right side of the lattice.

6.2 Analysis of the Ising model

For the analysis of the Ising model we define the magnetisation as

$$m = \frac{N_+ - N_-}{N} \tag{6.2}$$

N_+ represents the number of spins with the value $+1$ and likewise N_- represents the number of spins with the value -1. N is the total number of spins, which equals L^2 in our case. We shall now investigate how the magnetisation behaves as a function of temperature. We shall first do this for the model without a magnetic field and then we shall briefly see how our results change when we turn on a magnetic field.

6.2.1 Analysis of the Ising model without a magnetic field

The probability with which a particular state occurs is given by the Boltzmann factor $e^{-\beta \mathcal{H}}$, with $\beta = \frac{1}{k_B T}$ and k_B the Boltzmann constant. For $T = 0$ the system will therefore occupy a minimum energy state. This is accomplished when all spins are equal. Since there is no magnetic field, the configuration with all spins $+1$ and the configuration with all spins -1 yield the same minimal energy. The magnetisation is $+1$ and -1 respectively.

For $T \to \infty$, $\beta \to 0$, such that the Boltzmann factor equals 1 for every configuration. Then the values $+1$ and -1 are equally probable for each spin, such that $m \to 0$ for high temperatures. This is called the *disordered phase*.

One might expect a smooth curve between these two values, however the exact solution, found by Onsager in 1944, proves otherwise [3], [8]. Figure 6.2 shows the exact solution of the magnetisation as a function of temperature. We distinguish our discussed values for m at low and high temperatures. Furthermore, we note that there is a sharp drop at $T = T_c$, with T_c the *critical temperature*. This is the solution for the Ising model with an infinite number of spins. For a finite number of spins, the drop becomes less sharp. The sharp drop is called a *phase transition*, as we switch between two phases, one with random spin and one with equal spin. This phase transition occurs at $T_c \approx \frac{K}{0.44 k_B}$.

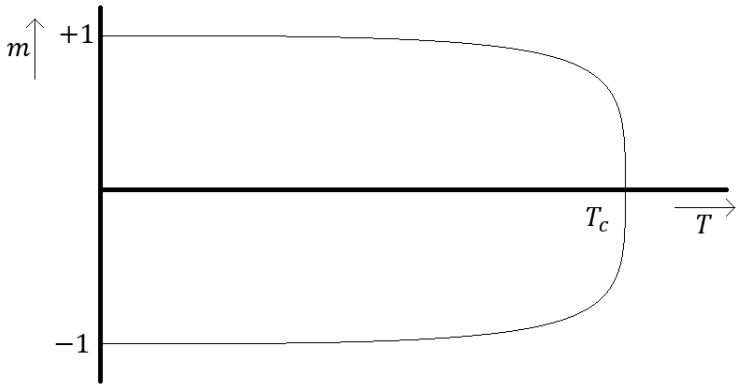

Figure 6.2: The exact solution of the magnetisation of the Ising model as a function of temperature without a magnetic field. The phase transition occurs at T_c. For temperatures above T_c the magnetisation equals zero.

6.2.2 Analysis of the Ising model with a magnetic field

Now we introduce a small positive magnetic field and see how the model changes. The second sum in Equation 6.1 starts to play a role. In the previous subsection we stated that there were two solutions for $T = 0$. Due to the second sum only the solution with $m = 1$ is stable. This means that we only get one curve as a solution. Another change occurs at the critical temperature. The transition becomes smoother instead of a sudden change as in Figure 6.2.

In the next subsection it is discussed how the Ising model can be simulated.

6.3 Simulating the Ising model

The simulating of the Ising model was done using a programming exercise from *Computational Physics* by J. Thijssen [12].

The simulating of the Ising model is done dynamically using time steps. Every time step consists of two stages. The configuration of the model at the beginning of the time step will be called the old configuration and is denoted by X. In the first stage of the model a trial configuration will be created, such that the trial and old configurations only differ by one spin. This trial configuration will be denoted by X'. A trial configuration is obtained by randomly selecting a site and changing its spin with respect to its spin value in the old configuration.

In the second stage it is determined whether the trial configuration will be accepted as the new configuration, otherwise the old configuration is kept as the new one. The difference in energy between the trial and old configuration determines whether the trial configuration is accepted. This difference in energy is denoted by

$$\Delta E(X \to X') = \mathcal{H}(X') - \mathcal{H}(X)$$

If $\Delta E(X \to X') < 0$ the trial configuration X' will be accepted. One might think that the trial configuration will never be accepted when $\Delta E(X \to X') > 0$, since the trial configuration is energetically unfavourable with regards to the old configuration. However, due to effects such as thermal fluctuation it is possible that the trial configuration is accepted. The probability of accepting the trial configuration, P_{accept}, is given by

$$P_{accept} = e^{-\beta \Delta E(X \to X')}, \qquad \Delta E(X \to X') > 0 \tag{6.3}$$

As $\Delta E(X \rightarrow X')$ increases, the acceptance probabilty decreases exponentially. In this model we never need E, or ΔE, by itself, only βE, or $\beta \Delta E$. Thus, we rewrite Eq. (6.1) as (assuming that the field $H = 0$)

$$\beta \mathcal{H} = -J \sum_{\langle i,j \rangle} s_i s_j$$

$J = \beta K$ is a new coupling constant which describes the interaction between two neighbours. Just like a critical temperature, as mentioned in subsection 6.2.1, there is a critical coupling constant J_c.

Consider the situation as in Figure 6.1. The selected site has one like neighbour and three different neighbours. If the spin is flipped then it has three like neighbours and one different neighbour. The energy difference is $-4J < 0$ thus in this case we would accept the trial configuration. If we change the situation slightly and consider a site with three like neighbours and one different neighbour, then the energy difference between the old and trial configuration would be $4J > 0$, so the probability of accepting the trial configuration is e^{-4J}.

The unit of time that is used in this model is Monte Carlo steps per spin (MCS). In stage 1 of the process a spin is chosen randomly. Since a square lattice with sides L is considered, the probability to select a specific spin is $\frac{1}{L^2}$. Thus, on average a spin is selected once every L^2 time steps. In the case of our model 1 MCS is equivalent to L^2 time steps. This is not a real time scale, however it does give some feeling to the process.

A starting configuration has to be chosen. Three options are to have all spins up, all spins down, or to start with a random configuration of spins. The last option would have approximately half of the spins up and the other half down. At the start of the simulation the system will move from the starting configuration to a stable configuration. What the stable configuration is, is determined by the temperature and the magnetic field. For low temperature and a small magnetic field there exist two stable configurations, all spins up or all spins down. When $T > T_c$ about half of the spins will be up and the other half will be down in equilibrium. This would result in a magnetisation of zero, which agrees with Figure 6.2. In general the system will spend some time to reach equilibrium. However, it is also possible that equilibrium is never reached. This occurs when the starting configuration and the equilibrium configuration are separated by a high free energy barrier.

6.4 Results of the Ising model

During the simulation once every MCS the current configuration was plotted. An example of a plot is shown in Figure 6.3.

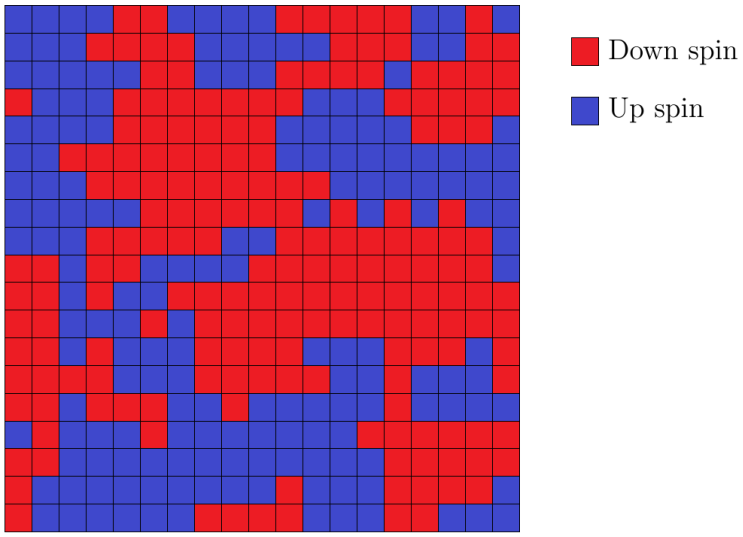

Figure 6.3: An example of a configuration of the 19×19 Ising lattice without a magnetic field. A red square corresponds to a down spin and a blue square corresponds to an up spin, -1 and $+1$ respectively. This simulation was done with $J = 0.4$.

An interesting aspect of the plot is that domains seem to form. This is expected, since it was stated in Section 6.1 that neighbouring sites favour like spins. As the simulation continues the domains change in form, but there are always domains. In Figure 6.3 the number of up and down spins is almost the same, so the magnetisation will be almost zero. However, during the process sometimes the up spins will dominate the lattice and sometimes the down spins will dominate the lattice. To show this the magnetisation has been measured during a simulation and it has been plotted as in Figure 6.4.

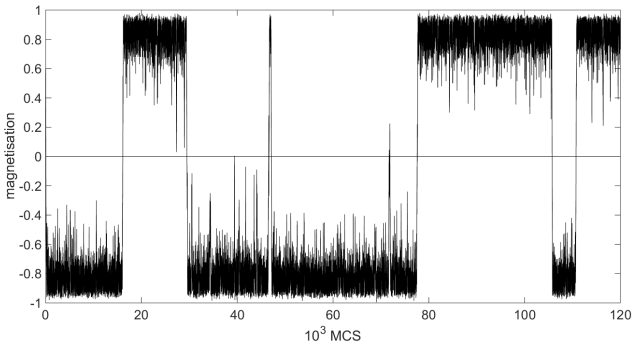

Figure 6.4: The magnetisation of a 19×19 Ising lattice as a function of time. $J = 0.46$ during the simulation.

6.5 Convergence of the Ising model

Section 5.3 discussed the convergence of a Monte Carlo method and offered a procedure to measure the convergence. This procedure shall be performed for the Ising model. We shall measure the energy during the simulation and use this data to obtain a certain time constant τ. A large τ indicates slow convergence and a small τ indicates fast convergence. τ will be determined for several sizes of the system, such that a relation between the size of the system and τ can be found.

The energy was fitted to an exponential using the fit function in Matlab. This fit function determines parameters a and b, such that the function $a \cdot e^{b \cdot t}$ is the best fit for the data. An example of a fit is shown in Figure 6.5.

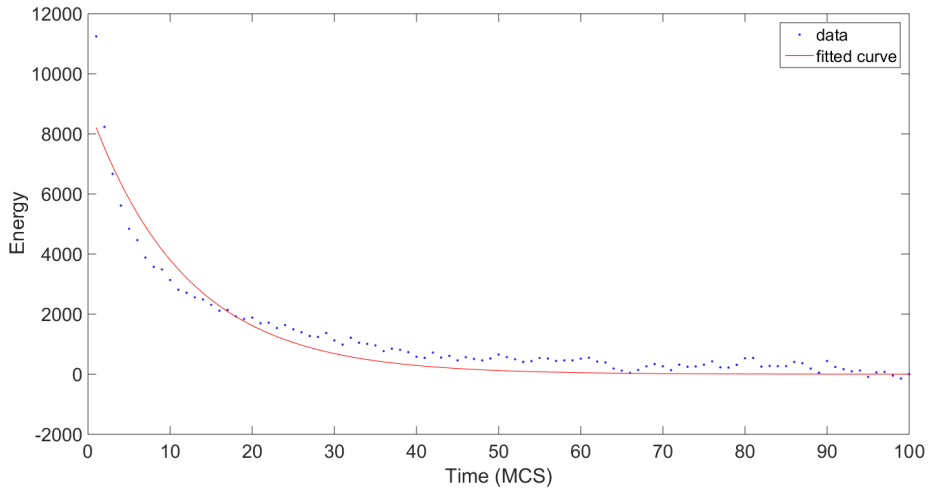

Figure 6.5: A fit of energy measured during a simulation of the Ising model. Only the first 100 MCS are shown, since this contains the information that is needed. The energy was adjusted, such that in equilibrium the energy will fluctuate around 0. This simulation was performed with $J = 0.46$

The relation between b and τ is given by

$$\tau = -\frac{1}{b} \tag{6.4}$$

For every size of the system 20 simulations were performed. All simulations were performed with $J = 0.46$. The chosen sizes are 100^2, 141^2 and 173^2. These were chosen because 141^2 is approximately twice as big as 100^2 and 173^2 is approximately three times as big as 100^2. A table showing the complete set of data can be found in the Appendix. The main results can be found in Table 6.1. The values stays approximately constant for the three different system sizes. However, they are all measured in MCS and the MCS also depends on the system size. For a system size N, 1 MCS equals N time steps. We conclude that the convergence scales linearly with the size of the system.

Normally, when every site on the lattice is influenced by all the sites on the lattice at least a quadratic relation between τ and the size of the system is to be expected. Thus, one could conclude that there is a certain domain around a spin which influences this spin, since there is only a linear relation between τ and the size of the system. The spins outside of this domain have no influence.

Table 6.1: The main results gathered from the data which can be found in the Appendix. For each system size 20 simulations were performed. b is a parameter for an exponential fit of the energy measured during a simulation. τ can be determined from b using Eq. (6.4)

	$N = 100^2$	$N = 141^2$	$N = 173^2$
Average value of b (MCS^{-1})	-0.07622	-0.07479	-0.07579
Standard deviation of b (MCS^{-1})	0.026755	0.012972	0.0152
τ (MCS)	13.1197	13.3704	13.1944

6.6 Conclusion of the Ising model

This concludes our first model, the Ising model. Since the Ising model is fairly easy to implement, it is a great starting point. It gives some ideas about phase transitions, how to ensure periodic boundary conditions and an overall understanding of these types of models. From here on more difficult models can be tackled. However, we then may face several difficulties. The main flaw is the type of lattice. For the model for describing the behaviour of adsorbed chlorine atoms on a Cu(111) surface, we should use a hexagonal lattice, instead of the square lattice we have seen in this chapter. The model of the next chapter, the hard hexagon model, shall use a triangular lattice which is still not correct, but is an improvement.

7 Hard hexagon model

The model discussed in this chapter, the hard hexagon model, presents a step forward modelling the adsorption process studied in this thesis. Just as in the previous chapter, we start with a description of the model. However, we do not analyse the hard hexagon model as we have done with the Ising model. The model has been solved by Baxter [3], but it is a rather difficult solution, so we will not discuss it here. We shall discuss how the model was implemented and discuss the results.

7.1 Description of the hard hexagon model

The hard hexagon model is formulated on a triangular lattice as shown in Figure 7.1. This is not the same as the hexagonal lattice which we shall consider in the final model. However, the fcc sites together form a triangular lattice and similar for the hcp sites. Thus in the hypothetical situation that chlorine atoms can only be adsorbed on fcc sites, or only on hcp sites, this lattice suffices. Therefore, the hard hexagon is closer to the problem we try to model than the Ising model.

As in the Ising model each site is labeled by i. Each site has the variable σ_i. σ_i can take the values 0 and 1. For an empty site $\sigma_i = 0$ and for an occupied site $\sigma_i = 1$. When using Boolean variables, so 0 corresponds to false and 1 corresponds to true, then σ_i states whether it is true or false that a site is occupied. When a site is occupied, so when $\sigma_i = 1$, we place a hexagon on the lattice as shown in Figure 7.1.

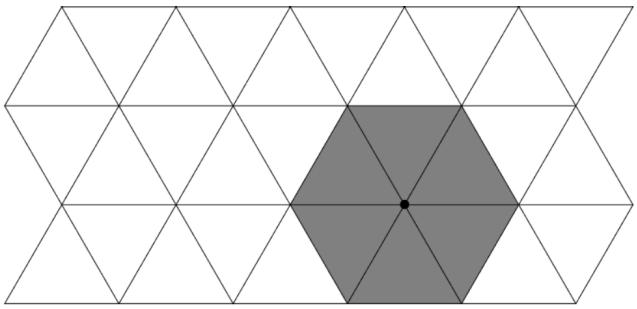

Figure 7.1: The triangular lattice as used in the hard hexagon model. When a site is occupied, a hexagon is placed on top of the lattice as shown.

Neighbouring sites are not allowed to both be occupied. So if a site is occupied, then its six neighbouring sites cannot be occupied. This is equivalent to stating that two hexagons are not allowed to overlap. This is the reason for the name of the model. Two configurations are shown in Figure 7.2. The left configuration has two atoms on neighbouring sites and thus two overlapping hexagons. This configuration is thus not allowed by the model. The right configuration has two touching hexagons, but since they do not overlap this configuration is allowed.

In the next section we shall first explain how the model is implemented when only requiring that hexagons do not overlap. Later we shall modify and extend the model such as to have it correspond to the experimental situation.

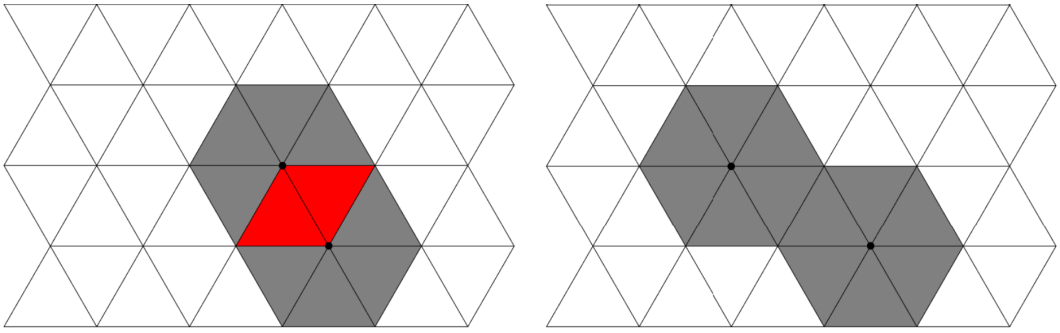

Figure 7.2: Two configurations of the hard hexagon model are shown. The left configuration is not allowed since two hexagons are overlapping. The right configuration is allowed, since the hexagons touch, but do not overlap.

7.2 Simulating the hard hexagon model

Simulating the behaviour of the hard hexagon is very similar to that of the Ising model. Again we first create a new configuration by selecting a random site. For the Ising model we then flipped the spin of the selected site, for the hard hexagon model we create a new configuration by placing an atom at the selected site. Then it is determined whether this new configuration is accepted. The Hamiltonian used in the Ising model had a coupling constant. For the hard hexagon model this coupling constant is infinite as neighbouring sites cannot both be occupied. However, there is a new parameter, the chemical potential. This chemical potential ensures that atoms will adsorb on a surface to lower their energy. We have previously seen in Figure 3.1 that the chlorine atoms form dense domains on the copper surface. This motivates the idea that a minimal energy is obtained by a close-packed system. If we strive for a close-packed system, we could accept every new configuration, as long as it does not violate the requirement that hexagons are not allowed to overlap. This shall be used as a first version of the model.

When a site is randomly selected, it has to be determined whether it is still available. It is available when itself and none of its neighbours are occupied. This can easily be done by creating two matrices, *occupied*, we denote it by O, and *available*, A. Both contain information for all the sites; O whether a certain site is occupied, and A whether a certain site is available. Every time step the matrices have to be updated. To do this quickly, it is useful to keep track of the neighbours for every site. This is again a matrix, we shall call it *neighbours*, N. The six neighbours of site i can be found in the ith row of N. N is filled before the simulation, since the neighbours are fixed for every site. Denote the number of sites as n, then O and A are vectors of length n and N is a $n \times 6$ matrix.

Two sites are shown in Figure 7.3, together with their six neighbours. The neighbours of site (2,2) ((i, j) is the site on row i and column j) are (1,2), (1,3), (2,1), (2,3), (3,2) and (3,3). In general for (i, j), with i even, the neighbours are $(i-1, j)$, $(i-1, j+1)$, $(i, j-1)$, $(i, j+1)$, $(i+1, j)$ and $(i+1, j+1)$. The neighbours of site (3,6) are (2,5), (2,6), (3,5), (3,7), (4,5) and (4,6). In general for (i, j), with i even, the neighbours are $(i-1, j-1)$, $(i-1, j)$, $(i, j-1)$, $(i, j+1)$, $(i+1, j-1)$ and $(i+1, j)$. As in the Ising model, periodic boundary conditions are used to ensure that the environment is the same for every site. To ensure this, modular arithmetic is used.

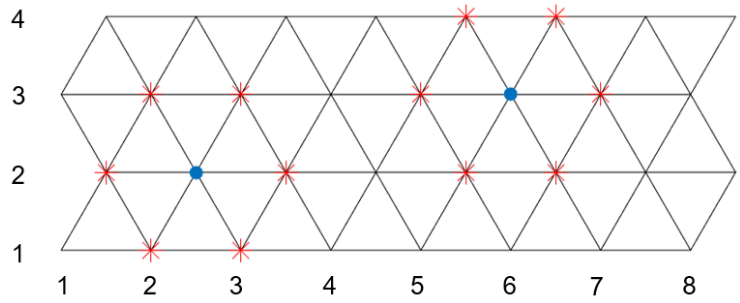

Figure 7.3: Two sites are selected, the left one is in the second row and the second column (2,2), the right one is in the third row and the sixth column (3,6). Note that the rows start from the bottom.

Figure 7.4 shows the result of this model. We note that there are regions in which the hexagons are packed as dense as possible, however there is a lot of space between the majority of the hexagons. This is caused by the fact that we always accept a new configuration, as long as there are no overlapping hexagons, although a denser configuration could be obtained by placing the hexagon on one of the neighbouring sites. This would yield a lower energy, due to the chemical potential.

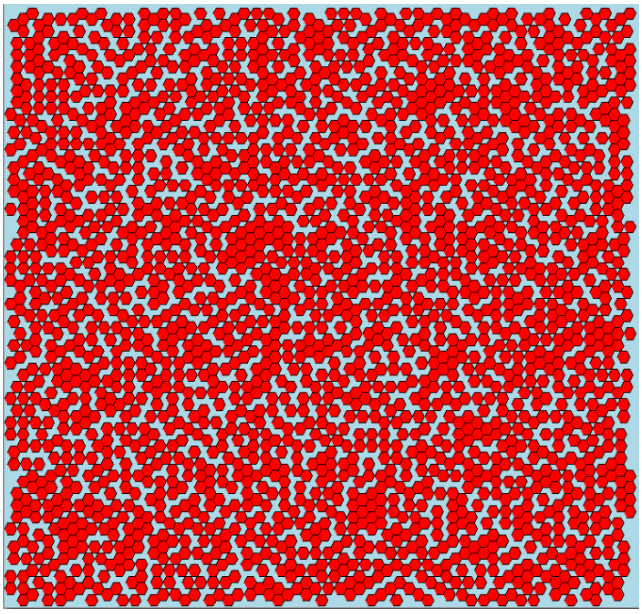

Figure 7.4: The result of the hard hexagon model when always accepting a new configuration as long as there are no overlapping hexagons.

In this model an atom is not allowed to diffuse or desorp after it has been adsorbed on the surface. Consequently, the model is stuck in a configuration in which the atoms are not densely packed. Including diffusion and desorption should fix this problem. Diffusion lets atoms move around on the surface. In one timestep an atom can only move to one of its neighbours, it cannot move several steps in one movement. This could be allowed, however we do not for simplicity. A crude visualization of the potential of the lattice can be seen in Figure 7.5. The atoms will be adsorbed on the wells. To diffuse on the surface, an atom has to move from one well to a neighbouring well. It has to overcome the barrier between these wells. The atom will be vibrating in a well and due to thermal fluctuations it will sometimes

have enough energy to overcome a barrier. This causes it to randomly move to one of the six neighbouring wells. If a site is occupied, then the well will turn into a hill, since another atom cannot be adsorbed on this site anymore. Consider a situation in which an atom is diffusing, but happens to move in the direction of a hill. Then it will not overcome the barrier and fall back into its old position. The atom does not know in advance that a site is unavailable, so it can try to move to this site, however it will fail to do so. Another process that could be implemented is desorption, however we shall see that implementing diffusion is already enough to give a good result.

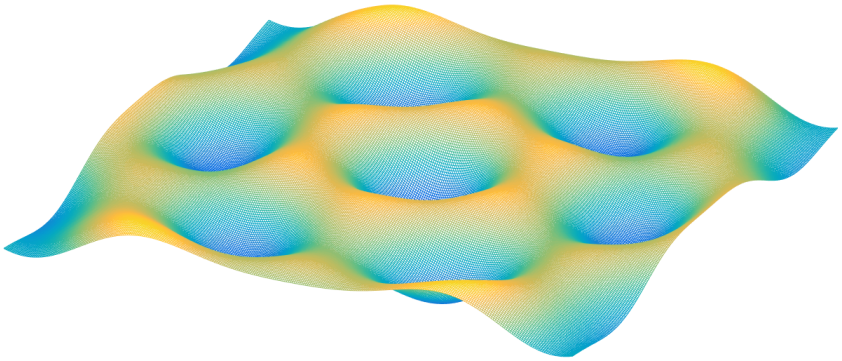

Figure 7.5: A crude way of visualizing the potential of the triangular lattice considered in the hard hexagon model. The atoms are adsorbed on the finite wells. To diffuse on the surface, an atom has to overcome the barrier between two wells.

The result of the new model is shown in Figure 7.6. Domains have formed in which the hexagons are as close-packed as possible. The boundaries between domains are formed by gaps.

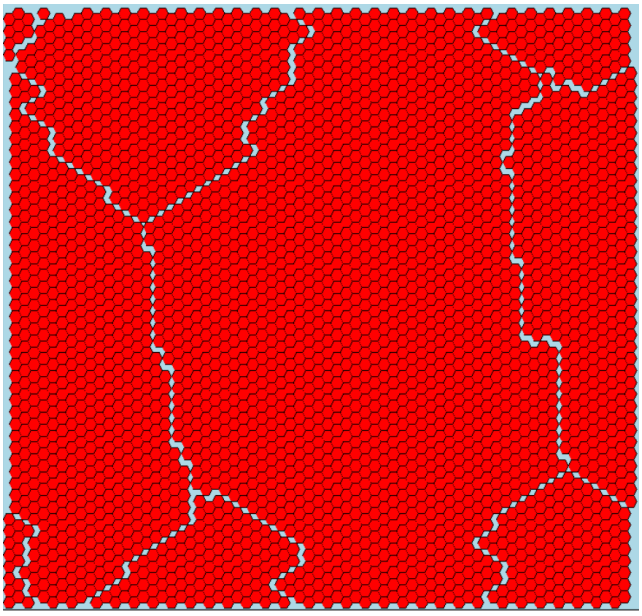

Figure 7.6: The result of the hard hexagon model when always accepting a new configuration as long as there are no overlapping hexagons. Diffusion has been added.

7.3 Conclusion of the hard hexagon model

In this chapter we have described and simulated the hard hexagon model. It serves as an introduction for the final model, which we are going to create in the next chapter. The hard hexagon model has introduced the adsorption and diffusion processes. Furthermore, this model is formulated on the triangular lattice, which is an improvement compared to the square lattice of the Ising model. However, a flaw is the interaction between the atoms on the surface. The range in the hard hexagon model is limited to neighbouring sites. In the final model we shall increase this range.

8 Model for the behaviour of adsorbed chlorine atoms on a Cu(111) surface

In the previous chapters we have considered two models, the Ising model and the hard hexagon model. For the problem we want to tackle the Ising model was very crude and the hard hexagon model still did not capture the full picture. In this chapter we try to create an accurate model for the behaviour of adsorbed chlorine atoms on a copper surface.

8.1 Description of the model

In the hard hexagon model a triangular lattice was used. If one solely considers the fcc sites or the hcp sites, then a triangular lattice suffices. However, we need to consider both the fcc sites and the hcp sites, so a hexagonal lattice as in Figure 2.6c will be used. As for the hard hexagon model we shall consider the adsorption and diffusion of chlorine atoms. Furthermore, we shall use the same process of selecting a site randomly and considering what process to execute. If a site is occupied, then diffusion is considered. If a site is unoccupied, then adsorption is considered. Both processes will not always be executed, this is determined by differences in energy of the old and trial configurations.

In Section 5.2 the process rates have been discussed. It was also mentioned that after each execution of a process, the process rates should be adjusted. In our case this happens naturally as in the beginning there are few occupied sites. When a site is randomly selected there is a high probability that it is unoccupied, thus adsorption will be considered. Later in the simulation many sites will be occupied, thus when a site is randomly selected there is a higher probability that diffusion is considered. During the simulation the rate of adsorption decreases, while the rate of diffusion increases. It was found that in the beginning the adsorption of atoms went too quickly. As a result the system did not have enough time to settle before a new atom was adsorbed. To solve this problem, an additional rate is added. For example, if this additional rate equals 0.05, then 1 of the 20 times an empty site is selected, adsorption will be considered.

The acceptance probabilities of trial configurations are calculated using a Hamiltonian as in Eq. (5.8). It is repeated here

$$\mathcal{H} = \sum_i n_i F_i^0 + \sum_{ij} V_{ij} n_i n_j + \sum_{ijk} V_{ijk} n_i n_j n_k + \dots$$

There exist two on-site energies, one for an fcc site and one for an hcp site. These energies can be found in Table 2.1. As previously stated, it has to be decided what types of interaction shall be taken into account. For this model we shall first only use two-point interaction. If necessary, three-point interaction can be added. Furthermore, it has to be decided which sites influence each other. We have chosen five different types of interaction, which can be seen in Figure 8.1. We assume that the influence of the sites beyond this range can be neglected. We shall refer to the type of interaction as seen in Figure 8.1a as J_1 and similarly, Figure 8.1b as J_2, Figure 8.1c as J_3, Figure 8.1d as J_4 and Figure 8.1e as J_5.

In an fcc domain, only J_5 interaction occurs. At the domain walls J_3, J_4 and J_5 interactions occur as can be seen in Figure 3.2. J_1 and J_2 have not been found experimentally, thus we conclude that these types of interaction cost too much energy. There are two options, either it is not allowed to have J_1 and J_2, or these are given such high energy that it is highly improbable that they occur. Both options have the same result, except in a high temperature regime where the probability to have J_1 or J_2 is not negligible anymore. We have chosen for a combination of the two options. It is impossible for a J_1 to occur, however it is possible to have a J_2 occur, although it comes with a high energy price.

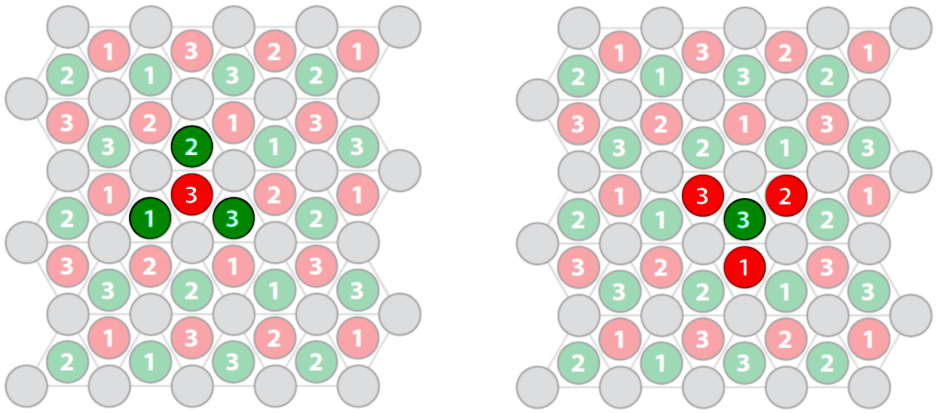

(a)

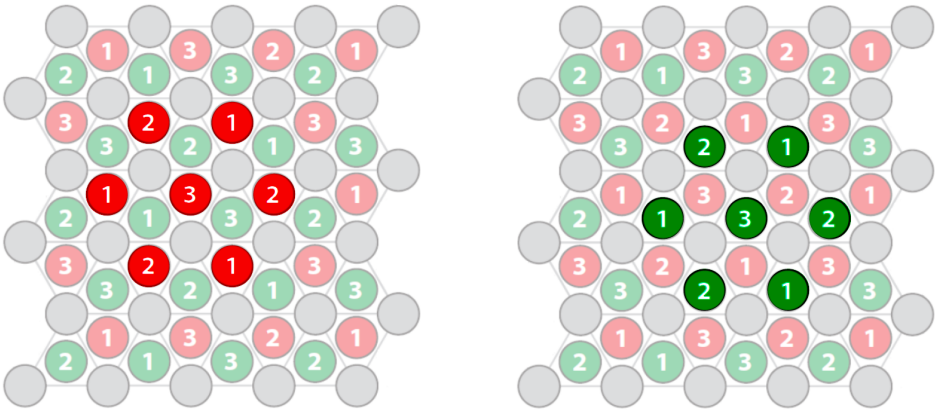

(b)

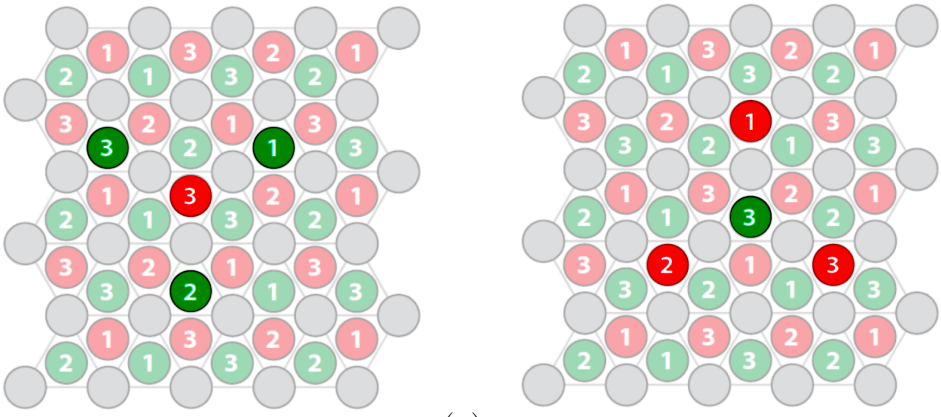

(c)

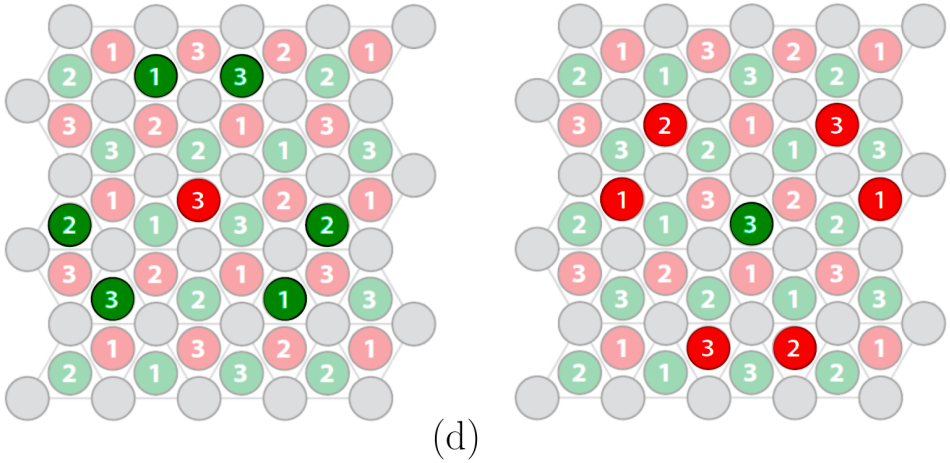

(d)

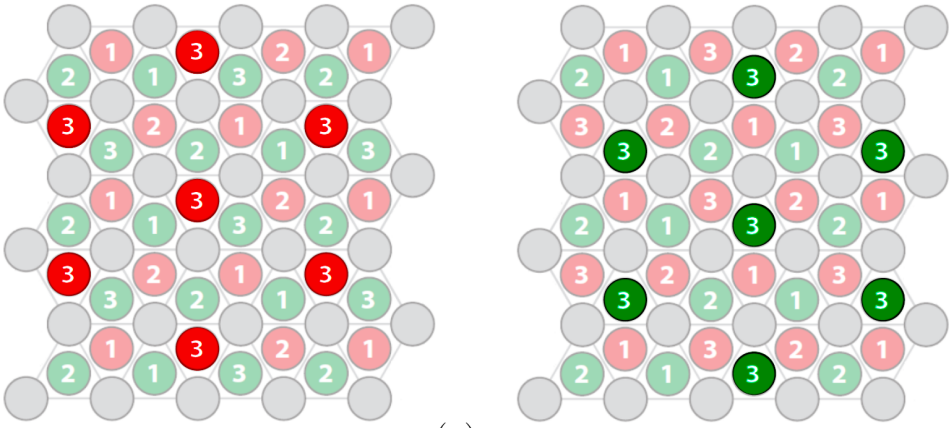

(e)

Figure 8.1: **(a)-(e)** The five types of interaction for fcc sites and hcp sites. The left column is for the fcc 3 site and the right column is for the hcp 3 site.

8.2 Acceptance probabilities

It has to be decided what energies shall be used for the types of interaction. Several energies can be found in two recent papers by T. V. Pavlova [9] and B.V. Andryushechkin [1], however these relate to two chlorine atoms on a Cu(111) surface, whilst we consider chlorine domains on a Cu(111) surface. These energies are thus not correct anymore, however they can be used as guidelines.

These energies will be used to calculate acceptance probabilities of trial configurations. The probability to accept a trial configuration considering adsorption is determined using a multiplication of the *fugacity*, $e^{-\beta\mu}$, with μ the chemical potential, a *site bias*, $e^{-\beta E_{site}}$, with E_{site} either the energy to be on an fcc site or the energy to be on an hcp site, and the weights relating to the different types of interaction, $e^{-\beta J_i}$, for interaction J_i. These weights occur n_{J_i} times, with n_{J_i} the number of J_i interaction that occur for the selected site. The adsorption probability is then given by

$$P_{adsorption} = e^{-\beta\mu} e^{-\beta E_{site}} \left(e^{-\beta J_2}\right)^{n_{J_2}} \left(e^{-\beta J_3}\right)^{n_{J_3}} \left(e^{-\beta J_4}\right)^{n_{J_4}} \left(e^{-\beta J_5}\right)^{n_{J_5}} \tag{8.1}$$

Consider the example in Figure 8.2. The selected site is an fcc site, so $E_{site} = E_{fcc}$. The

types of interaction that occur are: J_2, J_3, two times J_4 and two times J_5. The acceptance probability for this situation is

$$P_{accept} = e^{-\beta\mu} e^{-\beta E_{fcc}} e^{-\beta J_2} e^{-\beta J_3} \left(e^{-\beta J_4}\right)^2 \left(e^{-\beta J_5}\right)^2$$

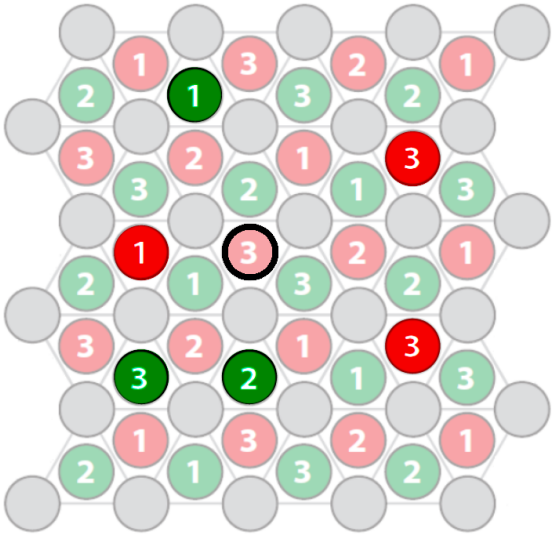

Figure 8.2: An example for calculating the probability to accept a trial configuration considering adsorption. The selected site is circled.

The probability to accept a trial configuration considering diffusion is determined using Eq. (8.2)

$$\begin{aligned} P_{diffusion} &= \frac{e^{-\beta E_{site}^{trial}} \left(e^{-\beta J_2}\right)^{n_{J_2}^{trial}} \left(e^{-\beta J_3}\right)^{n_{J_3}^{trial}} \left(e^{-\beta J_4}\right)^{n_{J_4}^{trial}} \left(e^{-\beta J_5}\right)^{n_{J_5}^{trial}}}{e^{-\beta E_{site}^{old}} \left(e^{-\beta J_2}\right)^{n_{J_2}^{old}} \left(e^{-\beta J_3}\right)^{n_{J_3}^{old}} \left(e^{-\beta J_4}\right)^{n_{J_4}^{old}} \left(e^{-\beta J_5}\right)^{n_{J_5}^{old}}} \\ &= \frac{P_{adsorption}^{trial}}{P_{adsorption}^{old}} \end{aligned} \tag{8.2}$$

This probability is determined by the energy for the position the chlorine atom was in first, the old configuration, and the energy for the new position, the trial configuration. We have chosen that a chlorine atom can only move to one of its nearest neighbours. A chlorine atom on an fcc site can move to one of the neighbouring hcp sites, and a chlorine atom on an hcp site can move to one of the neighbouring fcc sites as in Figure 8.1a. Take Figure 8.3 as an example. It is almost the same example as in Figure 8.2, except that the selected site of that example is now occupied and it can diffuse to the selected site in Figure 8.3. The selected site is an hcp site, so $E_{site} = E_{hcp}$. The types of interaction that occur are: J_2, J_3 twice J_4 and once J_5. The acceptance probability for this situation is

$$P_{accept} = \frac{e^{-\beta E_{hcp}} e^{-\beta J_2} e^{-\beta J_3} \left(e^{-\beta J_4}\right)^2 e^{-\beta J_5}}{e^{-\beta E_{fcc}} e^{-\beta J_2} e^{-\beta J_3} \left(e^{-\beta J_4}\right)^2 \left(e^{-\beta J_5}\right)^2} = \frac{e^{-\beta E_{hcp}}}{e^{-\beta E_{fcc}} e^{-\beta J_5}}$$

After these probabilities are determined, it has to be determined whether the trial configuration is accepted or not. This is done by taking a random number ρ between 0 and 1. If $\rho < P_{accept}$, then the trial configuration is accepted, otherwise it is not. It is possible that when calculating an acceptance probability, the outcome is greater than 1. It is of course impossible to actually have a probability greater than 1, however it is irrelevant to the simulation, since for all $P_{accept} \geq 1$ the trial configuration is always accepted, as wanted.

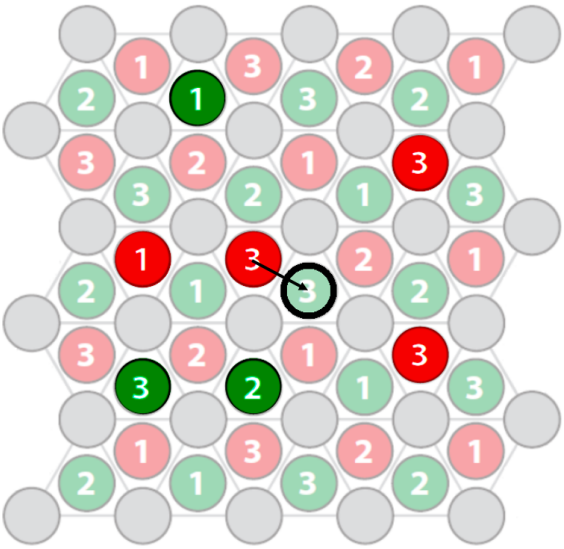

Figure 8.3: An example for calculating the probability to accept a trial configuration considering diffusion. The selected site is circled. The atom shall diffuse from an occupied site to the neighbouring selected site as indicated by the arrow.

Due to the fact that we do not allow for the J_1 interaction to occur, a site can be unoccupied, however unavailable for a chlorine atom to be adsorbed on or to diffuse to. As a result, it is possible that the probability to accept a trial configuration is zero.

8.3 First results of simulating the model

In this section we shall briefly discuss the first results of simulating the model as described in the previous sections. Figure 8.4 shows these results. We see that fcc domains form as expected. However, the domain walls that form are not as expected. The domain walls that have been found in our simulations always are straight lines, while the expected domain walls have more of a zig-zag pattern as can be seen in Figure 3.2. Another difference is the angle that the domain walls make with the horizontal. The walls found by N. Batenburg made an angle of 30°, 90° and 150° with the horizontal. The domain walls as in Figure 8.4d make an angle of 0°, 60° and 120° with the horizontal. After taking the rotational difference of the lattices into account, there is still a difference in the direction of the domain walls. Many different settings for $J_2, \ldots, J_5$ have been tried, but none have resulted in the correct domain walls. In the next section an analysis of the domain walls will be performed.

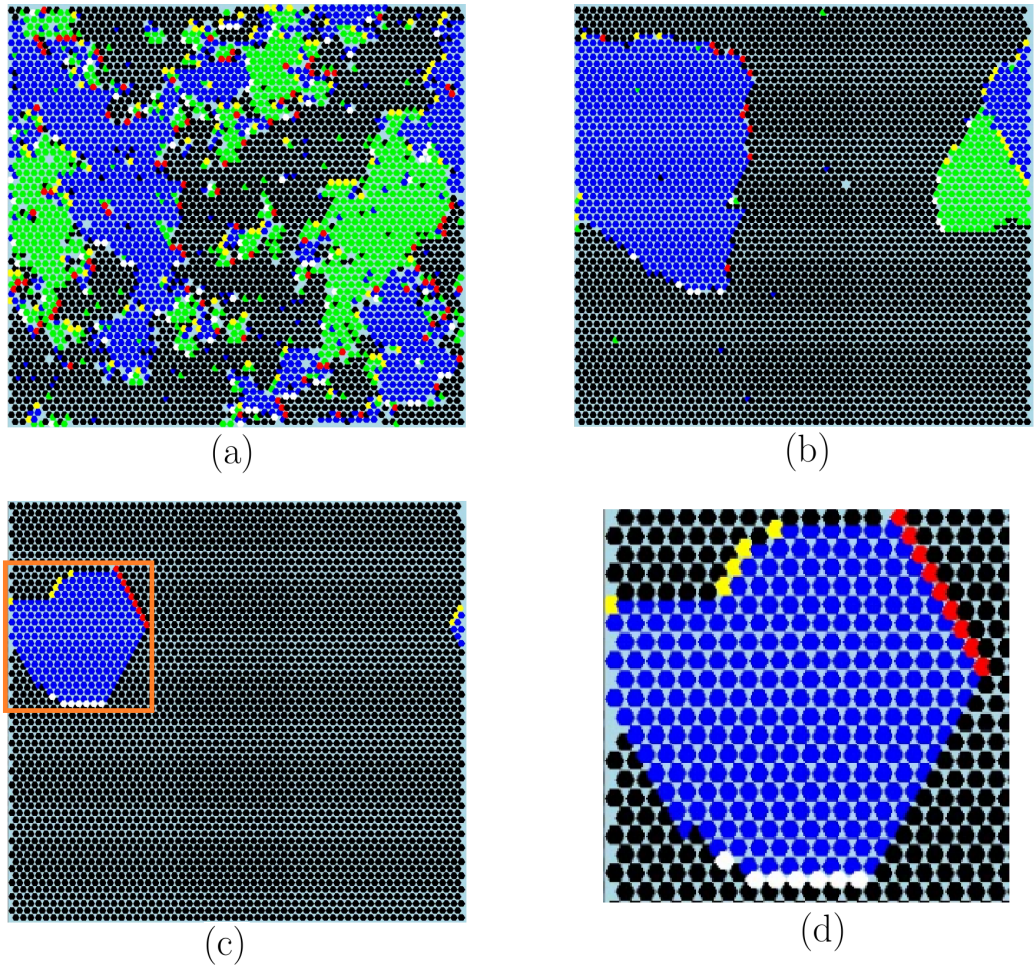

Figure 8.4: Six colors are used to indicate which type of site a chlorine atom occupies, blue corresponds to fcc 1, green corresponds to fcc 2, black corresponds to fcc 3, yellow corresponds to hcp 1, white corresponds to hcp 2 and red corresponds to hcp 3. The lattice in this figure is rotated 60 degrees with respect to the lattice we have seen previously in this thesis. (a) After a few MCS. Fcc domains have started to form, however the system is still mixed. (b) The system is not mixed anymore. There is a big domain which occupies the fcc 3 lattice. There are also smaller domains on the fcc 1 and fcc 2 lattice. Several atoms occupy the hcp lattice where the domains meet. (c) Near the end of the simulation, the domain on the fcc 3 lattice surrounds the domain on the fcc 1 lattice. (d) A crop corresponding to the orange square in (c). Small domain walls can be seen, formed by chlorine atoms on the hcp 1, 2 and 3 lattice.

8.4 Analysis of the domain walls

We have distinguished three types of domain walls that occur in our simulation and shall compare these to one of the domain walls found by N. Batenburg. These four cases of domain walls can be seen in Figure 8.5. For every type we shall calculate an energy density over the length of the domain wall.

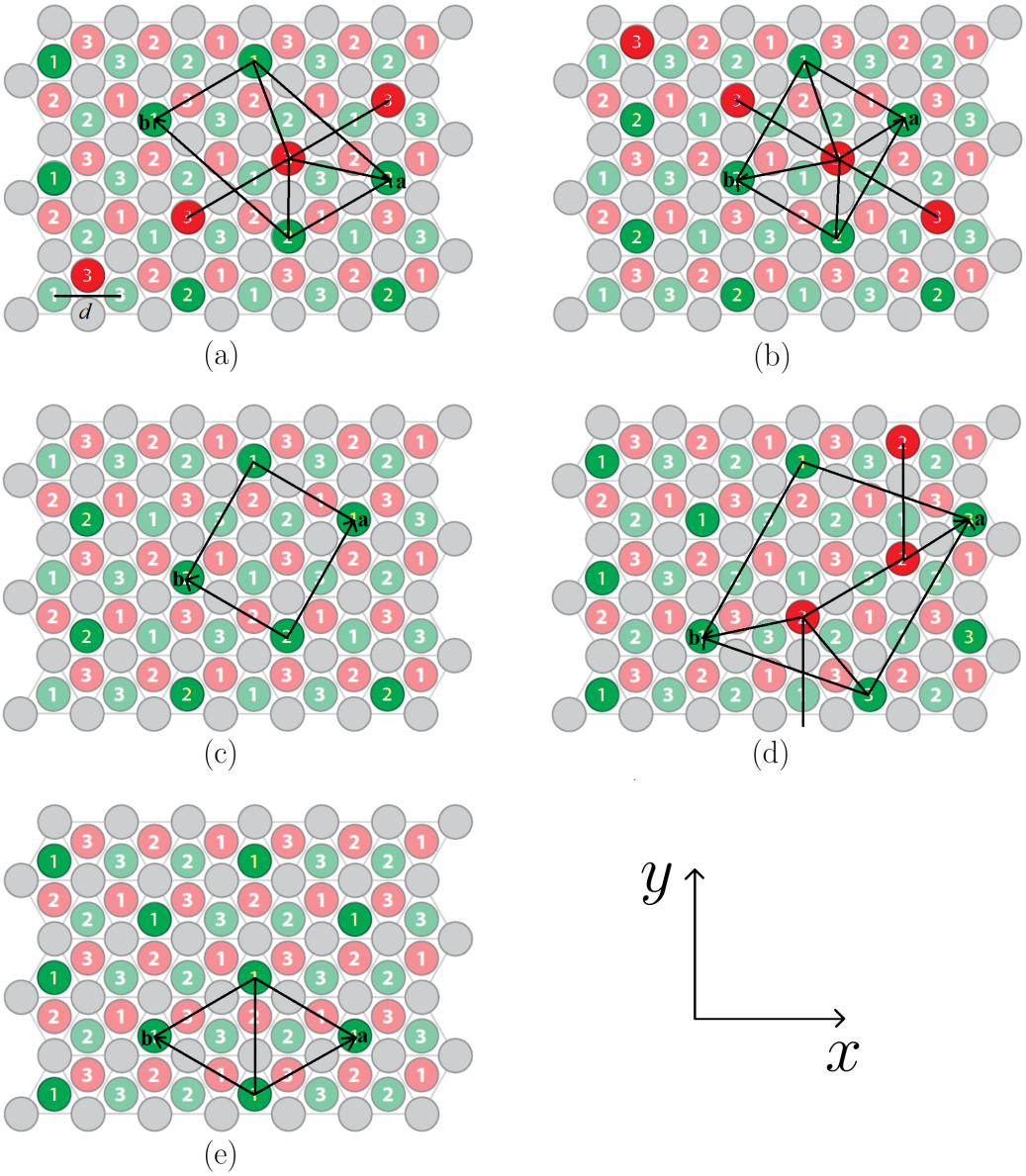

Figure 8.5: For each case the unit cells, lattice vectors and types of interaction are indicated. The x and y directions are also indicated. The distance between two fcc atoms is d as can be seen in (a). (a)-(c) Three cases found during simulations. (d) One of the domain walls as found by N. Batenburg. (e) A chlorine domain on the fcc 1 lattice. This will be used as a reference for the four cases in (a)-(d).

8.4.1 Reference energy

We first consider the reference energy density as in Figure 8.5e. In each unit cell there is one chlorine atom on an fcc site. We also have to subtract the chemical potential for this once. In each unit cell three J_5 occur. The lattice vectors are $\mathbf{a} = \frac{3}{2}d\hat{x} + \frac{1}{2}\sqrt{3}d\hat{y}$ and $\mathbf{b} = -\frac{3}{2}d\hat{x} + \frac{1}{2}\sqrt{3}d\hat{y}$, such that

$$\mathbf{a} \times \mathbf{b} = \left(\frac{3}{2}d\hat{x} + \frac{1}{2}\sqrt{3}d\hat{y}\right) \times \left(-\frac{3}{2}d\hat{x} + \frac{1}{2}\sqrt{3}d\hat{y}\right) = \frac{3}{4}\sqrt{3}d^2\hat{z} + \frac{3}{4}\sqrt{3}d^2\hat{z} = \frac{3}{2}\sqrt{3}d^2\hat{z}$$

The area of the unit cell is $\frac{3}{2}\sqrt{3}d^2$. The reference energy density per area is

$$\varrho_{ref} = \frac{E_{fcc} - \mu + 3J_5}{\frac{3}{2}\sqrt{3}d^2} \tag{8.3}$$

8.4.2 Case 1

In the unit cell of case 1, Figure 8.5a, one chlorine atom occupies an fcc site and one chlorine atom occupies an hcp site, we also have to subtract the chemical potential twice. Furthermore, there is one J_3, two J_4 and two J_5. One of the J_5 comes from the sides of the unit cell and the other one comes from the atoms on the hcp sites.

The lattice vectors are $\mathbf{a} = \frac{3}{2}d\hat{x} + \frac{1}{2}\sqrt{3}d\hat{y}$ and $\mathbf{b} = -2d\hat{x} + \sqrt{3}d\hat{y}$, such that

$$\mathbf{a} \times \mathbf{b} = \left(\frac{3}{2}d\hat{x} + \frac{1}{2}\sqrt{3}d\hat{y}\right) \times \left(-2d\hat{x} + \sqrt{3}d\hat{y}\right) = \frac{3}{2}\sqrt{3}d^2\hat{z} + \sqrt{3}d^2\hat{z} = \frac{5}{2}\sqrt{3}d^2\hat{z}$$

The area of the unit cell is $A_1 = \frac{5}{2}\sqrt{3}d^2$. The width of the unit cell (the distance from the domain on the fcc 1 lattice to the domain on the fcc 2 lattice) is $l_1 = \frac{5}{2}d$. The energy density per area for case 1 is

$$\varrho_1 = \frac{E_{fcc} + E_{hcp} - 2\mu + J_3 + 2J_4 + 2J_5}{\frac{5}{2}\sqrt{3}d^2} \tag{8.4}$$

8.4.3 Case 2

In the unit cell of case 2, Figure 8.5b, one chlorine atom occupies an fcc site and one chlorine atom occupies an hcp site, we again have to subtract the chemical potential twice. Two J_3, two J_4 and two J_5 occur. The lattice vectors are $\mathbf{a} = d\hat{x} + \sqrt{3}d\hat{y}$ and $\mathbf{b} = -\frac{3}{2}d\hat{x} + \frac{1}{2}\sqrt{3}d\hat{y}$, such that

$$\mathbf{a} \times \mathbf{b} = \left(d\hat{x} + \sqrt{3}d\hat{y}\right) \times \left(-\frac{3}{2}d\hat{x} + \frac{1}{2}\sqrt{3}d\hat{y}\right) = \frac{1}{2}\sqrt{3}d^2\hat{z} + \frac{3}{2}\sqrt{3}d^2\hat{z} = 2\sqrt{3}d^2\hat{z}$$

The area of the unit cell is $A_2 = 2\sqrt{3}d^2$. The width of the unit cell is $l_2 = 2d$. The energy density per area for case 2 is

$$\varrho_2 = \frac{E_{fcc} + E_{hcp} - 2\mu + 2J_3 + 2J_4 + 2J_5}{2\sqrt{3}d^2} \tag{8.5}$$

8.4.4 Case 3

In the unit cell of case 3, Figure 8.5c, one chlorine atom occupies an fcc site, so we have to subtract the chemical potential once. One J_5 occurs. The lattice vectors are $\mathbf{a} = \frac{3}{2}d\hat{x} + \frac{1}{2}\sqrt{3}d\hat{y}$ and $\mathbf{b} = -d\hat{x} + \sqrt{3}d\hat{y}$, such that

$$\mathbf{a} \times \mathbf{b} = \left(\frac{3}{2}d\hat{x} + \frac{1}{2}\sqrt{3}d\hat{y}\right) \times \left(-d\hat{x} + \sqrt{3}d\hat{y}\right) = \frac{3}{2}\sqrt{3}d^2\hat{z} + \frac{1}{2}\sqrt{3}d^2\hat{z} = 2\sqrt{3}d^2\hat{z}$$

The area of the unit cell is $A_3 = 2\sqrt{3}d^2$. The width of the unit cell is $l_3 = 2d$. The energy density per area for case 3 is

$$\varrho_3 = \frac{E_{fcc} - \mu + J_5}{2\sqrt{3}d^2} \tag{8.6}$$

8.4.5 Case 4

In the unit cell of case 4, Figure 8.5d, the domain wall as found by N. Batenburg, we again have one chlorine atom which occupies an fcc site. Two chlorine atoms occupy an hcp site, so we have to subtract the chemical potential three times. One J_3, two J_4 and one J_5 occur. The lattice vectors are $\mathbf{a} = \frac{3}{2}d\hat{x} + \frac{3}{2}\sqrt{3}d\hat{y}$ and $\mathbf{b} = -\frac{5}{2}d\hat{x} + \frac{1}{2}\sqrt{3}d\hat{y}$, such that

$$\mathbf{a} \times \mathbf{b} = \left(\frac{3}{2}d\hat{x} + \frac{3}{2}\sqrt{3}d\hat{y}\right) \times \left(-\frac{5}{2}d\hat{x} + \frac{1}{2}\sqrt{3}d\hat{y}\right) = \frac{3}{4}\sqrt{3}d^2\hat{z} + \frac{15}{4}\sqrt{3}d^2\hat{z} = \frac{9}{2}\sqrt{3}d^2\hat{z}$$

The area of the unit cell is $A_4 = \frac{9}{2}\sqrt{3}d^2$. The width of the unit cell is $l_4 = \frac{9}{2\sqrt{2}}d$. The energy density per area for case 4 is

$$\varrho_4 = \frac{E_{fcc} + 2E_{hcp} - 3\mu + J_3 + 2J_4 + 2J_5}{\frac{9}{2}\sqrt{3}d^2} \tag{8.7}$$

8.4.6 Comparing the cases

In the previous subsections we have calculated the energy density per area for the four cases and a reference energy density. Furthermore, the widths of the unit cells of the four cases have been determined. To compare the energy densities per length, Ξ, the reference energy density has to be subtracted from the energy densities of the four cases. This has to be multiplied by the width of the unit cells. We shall compare

$$\Xi_i = (\varrho_i - \varrho_{ref})\, l_i, \qquad i = 1, 2, 3, 4 \tag{8.8}$$

Comparing the Ξ_i was done using a brute force method of plugging in several values for E_{fcc}, E_{hcp}, J_3, J_4 and J_5. It was found that only for 'extreme' values, values which are far off from the expected value of E_{fcc}, E_{hcp}, J_3, J_4 or J_5, Ξ_4 had the lowest value. However, when these values were used during a simulation the domain walls found by N. Batenburg still did not form. Instead other configurations which were not considered during this analysis formed. We can conclude that in this version of the model, the domain walls found by N. Batenburg are energetically unfavourable compared to other types of domain walls, thus they will not appear in the simulations. In this version of the model, only two-point interaction was considered. As a modification we shall consider three-point interaction in the next section.

8.5 Three-point interaction

In the first version of the model we solely considered two-point interaction. This is the interaction between a pair of atoms. Three-point interaction is interaction between a trio of atoms. This type of interaction is weaker than the two-point interaction, however it can still have a great effect on the system. Consider the hypothetical situation in which state A and state B would have the same energy when only considering two-point interaction, but state A would have a higher energy than state B when three-point interaction is included. Both states will have the same probability of occuring when only considering two-point interaction, but including three point interaction increases the probability of state B occuring compared to state A occuring. It is possible that for our model, the domain walls found by N. Batenburg become energetically favourable when including three point interaction.

For the two-point interaction we had a maximum range of influence with J_5. We shall use the same range for the three-point interaction. For three atoms we shall use the combination of smallest two-point interactions possible. See Figure 8.6 for example. The atom on the left fcc 2 site has J_4 interaction with the atom on the hcp 3 site and J_5 interaction with the other

atom on the fcc 2 site. The atom on the other fcc 2 site has a J_3 and J_5 interaction. The atom on the hcp 3 site has a J_3 and a J_4 type interaction. For the three-point interaction we shall thus use J_3 and J_4 from the hcp 3 site, as this is the combination of the smallest two-point interactions. We shall refer to a three-point interaction consisting of the two-point interactions J_k and J_l as J_{kl}. Thus, the example of Figure 8.6 shall be referred to as J_{34}.

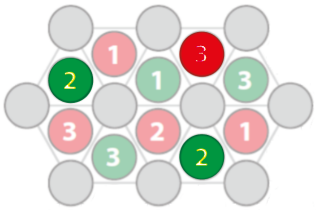

Figure 8.6: An example of the second version of J_{34}.

We shall only consider J_3, J_4 and J_5 as J_1 is not allowed to occur and J_2 seldom occurs. One could think that there are six types of three-point interaction, J_{33}, J_{34}, J_{35}, J_{44}, J_{45} and J_{55}. However, these only indicate which types of two-point interaction form the three-point interaction. Different version can exist due to a different angle between the two two-point interactions. For example, we have seen one version of J_{34} in Figure 8.6, but there is another version which can be seen in Figure 8.7.

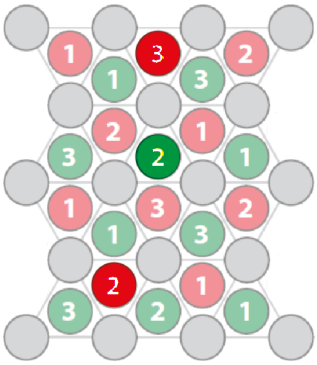

Figure 8.7: An example of the three point interaction J_{34}.

There is only one type of J_{33}, which can be seen in Figure 8.8.

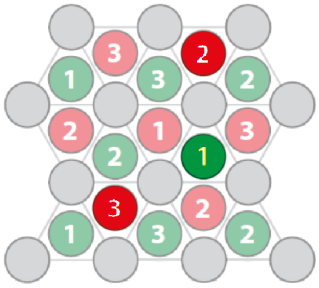

Figure 8.8: An example of J_{33}.

We have already distinguished two types of J_{34}, these are also the only types of J_{34}. To distinguish between the two types we shall refer to the one in Figure 8.7 as J_{34}^1 and to the one in Figure 8.6 as J_{34}^2.

There are two types of J_{35}, which can be seen in Figure 8.9. We shall refer to the left one as J_{35}^1 and to the right one as J_{35}^2.

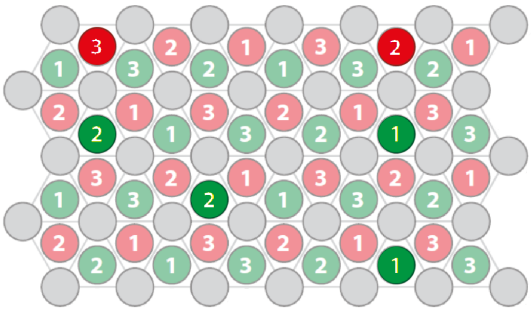

Figure 8.9: Examples of the two types of J_{35}.

There are five types of J_{44} and four types of J_{45}. We shall not show these in a figure.

There exist three types of J_{55}, which can be seen in Figure 8.10. The left one shall be referred to as J_{55}^1, the middle one as J_{55}^2 and the right one as J_{55}^3.

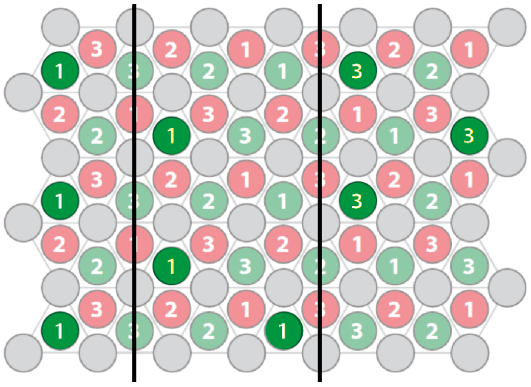

Figure 8.10: Examples of the three types of J_{55}. The different types have been separated by vertical lines.

The most interesting type of three-point interaction for our model is the J_{55}. The domain walls found during the simulation of the first version of the model, as in Figure 8.5a and b, are formed by atoms on a straight line of hcp sites. The domain walls as found by N. Batenburg, Figure 8.5d, form a zig-zag pattern. These are J_{55}^1 and J_{55}^2 respectively. J_{55}^3 occurs in the domains of chlorine atoms. By plugging in the right values of J_{55}^1 and J_{55}^2, the domain walls found by N. Batenburg may become energetically favourable compared to the domain walls found during the simulations of the first model.

Due to a lack of time, it has not been possible to thoroughly investigate the model with the three-point interaction included. Several values for the three-point interaction have been tried, but they did not yield the expected domain walls. With more time, more values can be tried. Furthermore, an analysis as in Section 8.4 could be performed to find a correct set of parameters.

It is also possible that three-point interaction is still not enough to accurately describe the process of chlorine adsorption on a Cu(111) surface. Maybe even more types of interaction have to be included, four-point interaction, five-point interaction, etcetera. However, as the influence of these types of interaction decreases, three-point interaction is weaker than two-point interaction and so on, this is not likely to solve the problem.

9 Conclusion and Outlook

The aim of this thesis was to create a model for the behaviour of adsorbed chlorine atoms on a Cu(111) surface, to better understand the domain boundary behaviour found by N. Batenburg [2].

Before this model was created the Monte Carlo method has been discussed and two models were investigated, the Ising model and the hard hexagon model. These models gave some insight into the behaviour of statistical mechanics models. Furthermore, an analysis of the convergence of the Ising model has been performed. It was found that the convergence increases linearly with the size of the system. This could indicate that there is a finite domain around a spin, which influences this spin. However, no further research has been performed, thus this conclusion is not necessarily true. For the final model first only two-point interaction was considered. However, it was found that two-point interaction is not enough to accurately describe the adsorption process. Thus three-point interaction was included. However, due to a lack of time, not enough research could be performed for the three-point interaction.

To create a more accurate model, further research for the three-point interaction should be performed. An analysis, as performed for the two-point interaction, can also be done for the three-point interaction. This should result in insight, whether it is possible or not to create an accurate model using two- and three-point interaction. Another approach would be to investigate the topology of the system. Screw dislocations were briefly mentioned in Chapter 3. Aspects of the system such as this one, have not been included in the model. It is possible that the topology of the system has to be included to create an accurate model.

References

[1] B. V. Andryushechkin, V. V. Zheltov, V. V. Cherkez, G. M. Zhidomirov, A. N. Klimov, B. Kierren, Y. Fagot-Révurat, D. Malterre, and K. N. Eltsov. Chlorine adsorption on cu (111) revisited: Lt-stm and dft study. *Surface Science*, 639:7–12, 2015.

[2] N. Batenburg. *Symmetry Breaking Domain Boundaries in a Chlorine Surface Reconstruction on Cu(111)*. TU Delft, 2016.

[3] R. J. Baxter. *Exactly solved models in statistical mechanics*. Elsevier, 1982.

[4] P. J. Goddard and R. M. Lambert. Adsorption-desorption properties and surface structural chemistry of chlorine on cu (111) and ag (111). *Surface Science*, 67(1):180–194, 1977.

[5] T. C. Hales. An overview of the kepler conjecture. *arXiv preprint math/9811071*, 1998.

[6] J. R. Hook and H. E. Hall. *Solid State Physics (The Manchester Physics Series)*. John Wiley and Sons Ltd, 1991.

[7] M. Kardar. *Statistical physics of fields*. Cambridge University Press, 2007.

[8] L. Onsager. Crystal statistics. i. a two-dimensional model with an order-disorder transition. *Physical Review*, 65(3-4):117, 1944.

[9] T. V. Pavlova, B. V. Andryushechkin, and G. M. Zhidomirov. First-principle study of adsorption and desorption of chlorine on cu (111) surface: Does chlorine or copper chloride desorb? *The Journal of Physical Chemistry C*, 120(5):2829–2836, 2016.

[10] M. Plischke and B. Bergersen. *Equilibrium statistical physics*. World Scientific Publishing Co Inc, 1994.

[11] J. Rogal. *Stability, composition and function of palladium surfaces in oxidizing environments: A first-principles statistical mechanics approach*. PhD thesis, Freie Universität Berlin Berlin, 2006.

[12] J. Thijssen. *Computational physics*. Cambridge university press, 2007.

Appendix: Results for the convergence of the Ising model

The table in this appendix contains all the results used for the convergence of the Ising model.

Table 9.1: The energy in the Ising model was measured during the simulation. Then it was fitted to an exponential of the form $a \cdot e^{b \cdot t}$. Using this b, the τ can be determined. This table contains the b values for 20 simulations for each of the three system sizes.

$N = 10^4$	$N = 141^2$	$N = 173^2$
-0.04202	-0.08454	-0.05504
-0.04728	-0.07762	-0.06993
-0.05758	-0.07337	-0.06503
-0.09773	-0.05367	-0.07343
-0.06766	-0.05139	-0.05692
-0.04705	-0.06143	-0.07981
-0.1186	-0.08915	-0.08407
-0.1029	-0.08211	-0.09333
-0.07256	-0.07208	-0.04446
-0.1091	-0.09092	-0.06432
-0.05209	-0.0655	-0.04282
-0.04919	-0.07803	-0.08463
-0.06121	-0.09351	-0.1065
-0.06877	-0.05498	-0.07034
-0.08811	-0.06883	-0.0828
-0.1304	-0.07678	-0.06408
-0.06947	-0.06071	-0.09548
-0.05938	-0.07051	-0.08464
-0.06733	-0.08681	-0.1127
-0.116	-0.1039	-0.08546